1521-0103/390/1/125–145$35.00
THE JOURNAL OF PHARMACOLOGY AND EXPERIMENTAL THERAPEUTICS
dx.doi.org/10.1124/jpet.123.002087
J Pharmacol Exp Ther 390:125–145, July 2024

High-dose Agomelatine Combined with Haloperidol Decanoate Improves Cognition, Downregulates MT2, Upregulates D5, and Maintains Krüppel-like Factor 9 But Alters Cardiac Electrophysiology

Sherine Abdelmissih, Marwa Abdelgwad, Doaa Mohamed Elroby Ali, Mohamed Sharif Ismail Negm, Mohamed Ali Eshra, and Amal Youssef

Departments of Medical Pharmacology (S.A., A.Y.), Medical Biochemistry and Molecular Biology (M.A.), Pathology (M.S.I.N.), and Medical Physiology (M.A.E.), Faculty of Medicine, Kasr Al-Ainy, Cairo University, Cairo, Egypt; and Department of Biochemistry and Molecular Biology, Faculty of Pharmacy, Sohag University, Sohag, Egypt (D.M.E.A.)

Received December 21, 2023; accepted May 2, 2024

ABSTRACT

Haloperidol decanoate (HD) has been implicated in cognitive impairment. Agomelatine (AGO) has been claimed to improve cognition. We aimed at investigating the effects of HD + low- or high-dose AGO on cognition, verifying the melatonergic/dopaminergic to the cholinergic hypothesis of cognition and exploring relevant cardiovascular issues in adult male Wistar albino rats. HD + high-dose AGO prolonged the step-through latency by +61.47% ($P < 0.0001$), increased the time spent in bright light by +439.49% ($P < 0.0001$), reduced the time spent in dim light by –66.25% ($P < 0.0001$), and increased the percent of alternations by +71.25% ($P < 0.0001$), despite the reductions in brain acetylcholine level by –10.67% ($P < 0.0001$). Neurodegeneration was minimal, while the mean power frequency of the source wave was reduced by –23.39% ($P < 0.05$). Concurrently, the relative expression of brain melatonin type 2 receptors was reduced by –18.75% ($P < 0.05$), against increased expressions of dopamine type 5 receptors by +22.22% ($P < 0.0001$) and angiopoietin-like 4 by +119.18% ($P < 0.0001$). Meanwhile, electrocardiogram (ECG) demonstrated inverted P wave, reduced P wave duration by –36.15% ($P < 0.0001$) and PR interval by –19.91% ($P < 0.0001$), prolonged RR interval by +27.97% ($P < 0.05$), increased R wave amplitude by +523.15% ($P < 0.0001$), and a depressed ST segment and inverted T wave. In rats administered AGO, HD, or HD+ low-dose AGO, Alzheimer's disease (AD)-like neuropathologic features were more evident, accompanied by extensive ECG and neurochemical alterations. HD + high-dose AGO enhances cognition but alters cardiac electrophysiology.

SIGNIFICANCE STATEMENT

Given the issue of cognitive impairment associated with HD and the claimed cognitive-enhancing activity of AGO, combined high-dose AGO with HD improved cognition of adult male rats, who exhibited minimal neurodegenerative changes. HD+ high-dose AGO was relatively safe regarding triggering epileptogenesis, while it altered cardiac electrophysiology. In the presence of low acetylcholine, the melatonergic/dopaminergic hypothesis, added to angiopoietin-like 4 and Krüppel-like factor 9, could offer some clue, thus offering novel targets for pharmacologic manipulation of cognition.

Introduction

Over time, the cholinergic deficiency hypothesis culminating in cognitive and memory disruptions has proven realistic when memory-enhancing medications relied on increasing acetylcholine (ACh) (Baxter and Crimins, 2018). Unlike the early reduction in ACh levels, the involvement of acetylcholinesterase (AChE), the ACh metabolizing enzyme, seemed to occur relatively late (Perini et al., 2002). Among neurotransmitters implicated as modifiers of cholinergic signaling is melatonin, which was able to prevent the inhibition of ACh synthesizing enzyme in several neuronal proteins (Guermonprez et al., 2001). Durand-de Cuttoli et al. (2018) discussed dopamine interactions with ACh in modifying multiple brain functions, including cognitive performance. Furthermore, dopamine type 5 receptors (D5) were claimed to assist the role of ACh in maintaining healthy learning and memory processes (Rizzi and Tan, 2017).

The link between some antipsychotic medications, sleep issues, and dementia, with subsequent progressive neurodegeneration and cognitive impairment, were previously explored (Pillai and Leverenz, 2017; Xu et al., 2020). Regular monthly injections of the depot form of haloperidol, haloperidol decanoate

This research did not receive any specific grant from funding agencies in the public, commercial, or not-for-profit sectors.
The authors declare that there are no conflicts of interest.
dx.doi.org/10.1124/jpet.123.002087.

ABBREVIATIONS: ACh, acetylcholine; AChE, acetylcholinesterase; AD, Alzheimer's disease; AF, atrial fibrillation; AGO, agomelatine; ANGPTL4, angiopoietin-like 4; bpm, beats per minute; D5, dopamine-5 receptors; ECG, electrocardiogram; EEG, electroencephalogram; HD, haloperidol decanoate; HR, heart rate; KLF9, Krüppel-like factor 9; MT2, melatonin type 2 receptors; TpTe, T peak-Tend.

(HD), results in the slow release of free haloperidol into the systemic circulation. Warnings have been issued regarding the use of HD in cases of neurologic and cardiac disorders, including some types of dementia, cerebrovascular stroke, arrhythmia, and heart failure. In rodent studies, HD precipitated QTc prolongation, and increasing the dose of HD to 1 mg/kg or above precipitated ventricular arrhythmia. The induced cardiac adverse effects seemed of interest based on the reported link between cardiovascular issues and cognitive defects (Liang et al., 2021). However, off-label use of haloperidol in patients with dementia-associated agitation and psychotic features is still adopted (Mühlbauer et al., 2021).

In clinical practice, HD can be coadministered with hypnotics and/or antidepressants to alleviate some of the antipsychotics-associated adverse effects such as agitation, depression, and insomnia (Haldol decanoate Package Leaflet 2020). Agomelatine (AGO), a hypnotic and antidepressant drug, acts as a nonselective melatonin [melatonin type 1 receptor and melatonin type 2 receptor (MT2)] agonist and a serotonin 5-HT_{2C} receptor antagonist (Gobbi and Comai, 2019). Unlike other antidepressants, AGO exerts an additional anxiolytic activity (Yohn et al., 2017) and was considered a favorable hypnotic in terms of its claimed enhancing effect over learning and memory, in addition to its neuroprotective properties (Gupta et al., 2015). Hence, AGO has been suggested as a potential treatment for the cognitive defects and psychotic features associated with low muscarinic signaling in human psychoses and animal models of schizophrenia (Barak and Weiner, 2009).

As cerebrovascular disorders were implicated in cognitive deficits (Hedges et al., 2019), recently, angiopoietin-like 4 (ANGPTL4), a member of the angiogenic-regulating secreted protein superfamily (Zhu et al., 2012), which plays a key role in angiogenesis, was found to serve as a diagnostic biomarker in patients with clinically assessed vascular-related cognitive defects (Chakraborty et al., 2018). Currently, research on the implication of ANGPTL4 in neurologic disorders is ongoing.

Identified as a required regulator of central nervous system and neuronal maturation (Pollak et al., 2018), Krüppel-like factor 9 (KLF9) is a member of the novel Krüppel-like factor family of evolutionarily conserved zinc finger transcription factors (Wang et al., 2008). Targeting KLF9 was able to improve stress-provoked depression, as well as other related behavioral issues (Besnard et al., 2018). KLF9 was also linked to cardiac ischemia (Yan et al., 2019). Up until now, the involvement of KLF9 in neuronal dysfunctions remains an obscure area of research interest.

Therefore, the diversity of factors affecting cognition drew our attention to conduct our experiment, where we aimed at comparing the effects of long-term combined HD + AGO on cognition. Conducting behavioral tests, while analyzing the brain's electrical signals, with special emphasis on beta and delta wave activities, being closely linked to cognition as well as to each other (Harmony, 2013; Jang et al., 2019), together with histopathologic examination were integral parts of our assessments. The electrical activity of the heart was recorded as well to identify any relevant cardiovascular issues. The cholinergic deficiency hypothesis of cognition was verified against the melatonergic/dopaminergic hypothesis. ANGPTL4 and KLF9 were investigated as respective novel mediators of brain vascularization and neuroregeneration. Secondarily, we aimed at discriminating between two commonly used AGO doses in research. The presumptive cognitive, neuropathological, biochemical, and cardiac outcomes of our experiment would have important clinical implications by offering novel cognitive enhancers and/or raising awareness about combined HD + AGO use, taking into consideration the balance between benefit and risk potentialities.

Materials and Methods

Experimental Design and Treatments

All experimental procedures comply with the ARRIVE guidelines and were carried out in accordance with the National Research Council's Guide for the Care and Use of Laboratory Animals. Animals' housing, handling, and experimentation were approved by the Institutional Animal Care and Use Committee of Cairo University (CU/III/F/53/22). Adult male Wistar albino rats aged 7 to 8 months (200–250 g) were obtained from Animal House of Faculty of Medicine, Kasr Al-Ainy, Cairo University. Animals were maintained at six rats/cage in the Acclimatization Room at the Medical Pharmacology Department, Faculty of Medicine. Kasr Al-Ainy, Cairo University for 7 days before the start of the experiment, under standard conditions (22±2°C room temperature; 45%–50% relative humidity; 12-hour light/dark cycle with lights on at 07:30), with free access to food and water. Training sessions, drug administration, as well as behavioral tests were conducted between 10:00 and 16:00.

To investigate the long-term effects of HD and/or AGO (low and high dose) on cognition, rats ($n = 42$) were divided equally into the following seven groups: 1) control group [10 mL/kg distilled water (DW), oral]; 2) corn oil-treated group (0.08 mL/kg corn oil, deep intramuscular at back of thigh); 3) low-dose AGO (Sigma-Aldrich Co., Ltd, USA) (40 mg/kg, oral); 4) high-dose AGO (80 mg/kg, oral) (Can et al., 2018); 5) HD (Sigma-Aldrich) (4 mg/kg, deep intramuscularly at back of thigh) (Debonnel et al., 1990; He et al., 2017); 6) HD (4 mg/kg deep IM) + low-dose AGO (40 mg/kg, oral); and 7) HD (4 mg/kg deep i.m.) + high-dose AGO (80 mg/kg, oral). HD was dissolved in corn oil, while AGO was suspended in distilled water (Veronesi et al., 2021). All treatments were administered once daily for 6 weeks. HD was administered once weekly. No pharmacokinetic interactions were previously reported between HD and AGO; however, on days when rats were to receive both drugs, we preferred to administer oral AGO prior to the deep intramuscular injection of HD, to avoid any minor agony resulting from the HD injection that would make rats uncomfortable when handled to receive AGO by oral gavage. On the last day of the experiment, rats were dosed and weighed, then behavioral assessments were done, followed by electroencephalogram (EEG) and electrocardiogram (ECG) of the sedated animals. Subsequently, rats were sacrificed by decapitation under intravenous ketamine anesthesia, followed by brain dissection. Brains were halved into right and left brain hemispheres, and each brain hemisphere was weighed.

Behavioral Assessments of Cognition

Dim to Bright Light Preference Test (Derived from Passive Avoidance Test). One square glass box, measuring 30 cm × 30 cm × 30 cm (length × width × height), was divided into two partitions by a manually removable opaque barrier. The smaller compartment (10 cm × 30 cm × 30 cm) was transparent to room lights, and the other larger partition (20 cm × 30 cm × 30 cm) was surrounded by an opaque box with one open side (the side toward the smaller partition). For exploration and learning, training was conducted by transferring rats, one cage at a time, to the laboratory room to be left without intervention for 30 minutes. Afterward, one rat was placed in the smaller illuminated partition of the glass box, out of sight from the other rats, where the animal was allowed to explore for 30 seconds; then the manual barrier was removed, and the rat was allowed to wander freely, transitioning between bright and dim light partitions for 5 minutes. This was repeated three times, at 15-minute intervals. Each time the rat entered the dim light compartment, a brief and sudden

pinprick was applied to its back. After the third test trial and once the rat left the dim light partition, the barrier was put back and the rat was left for 10 seconds in the bright light chamber, followed by its return to the home cage. This was repeated on 2 successive days (Fig. 1). After a retention period of 24 hours to assess short-term memory, each individual rat was replaced in the light compartment and permitted to enter the dark partition; testing was conducted in the absence of the painful stimulus. The time (in seconds) until the first complete entry into the dim light chamber with all four paws was taken as the "step-through latency." The total time allowed for exploration of both partitions was 180 seconds (3 minutes), and the percent of time (in seconds) spent in each of the bright and dim light chambers was calculated (Rao Barkur and Bairy, 2015).

Y-Maze Test. The Y-maze test was used to assess spatial working and recognition memory. It consisted of three equally spaced arms (each 120°, 20 cm long, 13 cm wide, and 20 cm high), labeled A, B, and C, converging in an equilateral triangular central zone of 15 cm at its longest axis (Roghani et al., 2006). Each rat was placed in arm B, facing the center, while all three arms were opened. The rat was permitted to move freely for 5 minutes. Arm entry was considered when all four paws were completely inside one arm with the rat's snout facing the end of the arm (Miedel et al., 2017). The sequence of arm entries was manually recorded and the number of alternations, defined as consecutive entries in all three arms, was also counted. The percent of alternations was calculated [(Number of spontaneous alternations/Maximum alternations (Total number of arms entered – 2)) × 100] (Onaolapo et al., 2012), as were the total distance traveled in the maze within each arm and within the central zone and the number of entries per arm. The apparatus was cleaned with 70% ethanol and water between individual rats (Miedel et al., 2017).

Electrophysiologic Recordings

Electroencephalography. Following the behavioral assessments, EEG was performed during the daytime and for 5 minutes per rat, with animals sedated using single 350 mg/kg intraperitoneal of 10% chloral hydrate. EEG recording was accomplished in sedated rats with closed eyes using the data acquisition system PowerLab 4/30 (ML866, ADInstruments, Australia), Animal BioAmp (ML136, ADInstruments), and Laboratory Chart software v7.2. Subdermal scalp needle electrodes (MLA1203; ADInstruments) were inserted according to the manufacturer's brochure (ADInstruments). Recordings were performed at a sampling rate of 1 kHz, at 500 μV range, high-pass filter of 0.1 Hz, low-pass filter of 200 Hz, and with mains-filter on. Source EEG signal, recorded on channel 1, was filtered to beta, as were delta rhythms (channels 2 and 3), using the same sampling rate and range, with the respective bandpass filters of 12 to 30 and 0.5 to 4 Hz. Offline global power analysis was applied. Total EEG power (V^2), mean power frequency (Hz), and mean EEG amplitude (μV), of source, beta, and delta waves were obtained and illustrated on different channels. The spike discriminator was set up to detect bipolar spikes at a fit tolerance of 20 μV and peak at 50 μV, with time from 1 millisecond to 1000 milliseconds, and was used to illustrate mean EEG amplitude. To compare amplitudes of different EEG waves, the absolute numerical values were adopted in statistical analysis.

Electrocardiography. Following EEG recordings, ECG was performed using the data acquisition system PowerLab 4/30 (ML866, ADInstruments) during the daytime and for 5 minutes per rat, at a sampling rate of 4 kHz, 20 mV range, high-pass filter of 0.3 Hz, low-pass filter of 1 kHz, and with mains-filter on, according to the manufacturer's brochure (ADInstruments). Offline analysis was done on input channel 1 (source channel), to obtain data for heart rate (HR) [beats per minute (bpm)]; amplitudes (millivolts) of P, Q, R, S, ST, and T waves; and duration (milliseconds) of P wave, PR interval, QRS complex, QT, QTc, JT, T peak-Tend (TpTe), and RR intervals. Averaging view was preset at rat ECG values and set to average 10 beats (P wave = atrial contraction; PR interval = atrio-ventricular conduction; Q wave = the negative deflection that precedes the R wave; R wave = positive upward deflection that follows the Q wave;

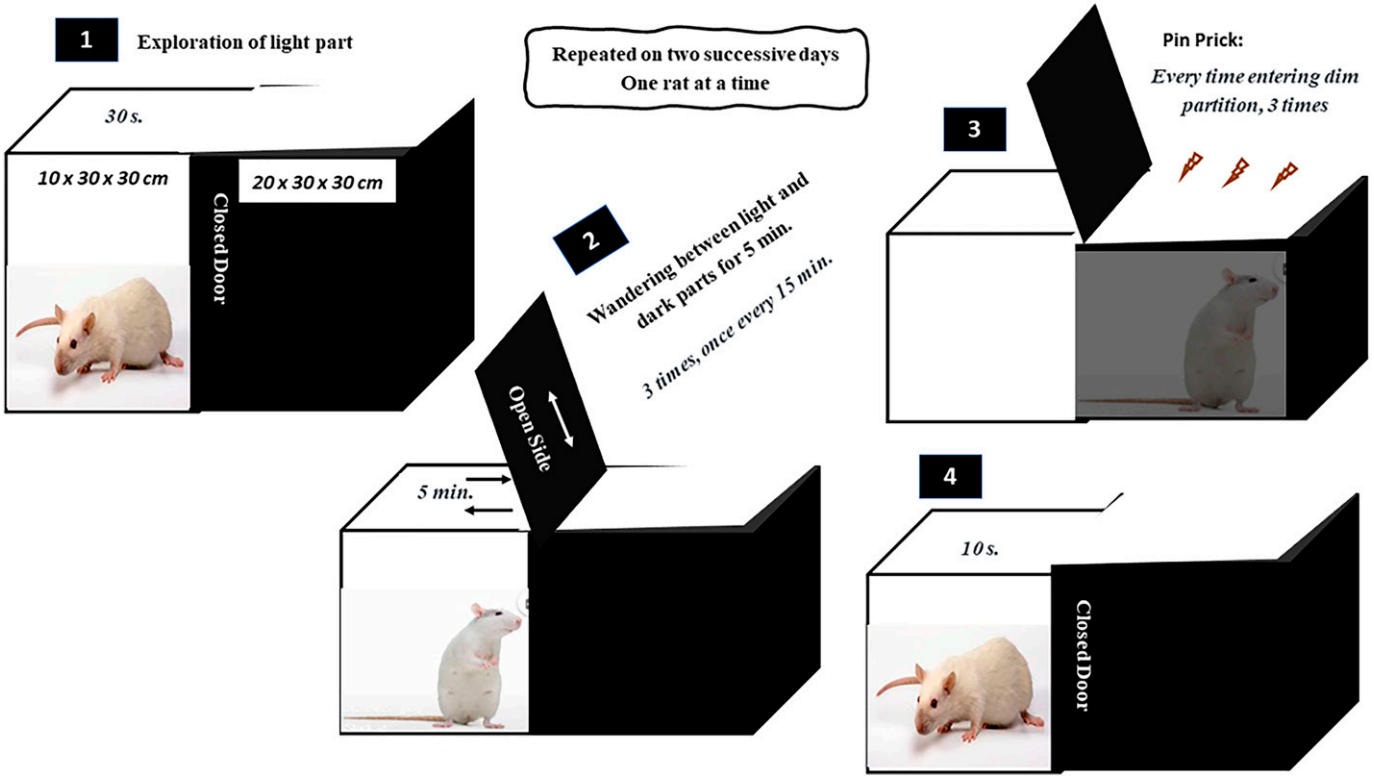

Fig. 1. Sequence of events in training session for the dim to bright light preference of adult male Wistar albino rats subdivided into control (oral DW or i.p. corn oil), low-dose AGO (oral 40 mg/kg), high-dose AGO (oral 80 mg/kg), HD (i.p. 4 mg/kg, once weekly), HD + low-dose AGO, and HD + high-dose AGO.

S wave= small negative wave following the R wave; QRS = duration of ventricular contraction; T wave = ventricular relaxation; QT = time from start of ventricular contraction until the end of ventricular relaxation; QTc = time from start of ventricular contraction until the end of ventricular relaxation (corrected for heart rate); J wave = point at the end of QRS; JT interval = ventricular repolarization, from end of ventricular contraction (QRS) until the end of ventricular relaxation; ST segment = the interval between ventricular depolarization and ventricular repolarization (line between J point and start of T wave); Tpeak-Tend = transmural dispersion of ventricular repolarization. To compare amplitudes of different ECG waves, the absolute numerical values were adopted in statistical analysis.

Body Weight and Weights of Right and Left Brain Hemispheres

At the end of the study, rats' body weights (g) were assessed. Following the behavioral assessments and electrophysiologic recordings, rats were euthanized by decapitation under intravenous ketamine anesthesia, brains were dissected, and then each hemisphere was separated and weighed (g).

Pathologic Assessment

The rats' brains were immersed in 10% formalin then processed in alcohol and xylene and embedded in paraffin blocks. Two sections were cut at 5 microns by Leica cryostat; one was stained with H&E, while the other was stained with Congo Red stain. The digital images of the selected tissue preparations were photographed using Olympus DP26 digital net camera attached to an Olympus CX31 microscope. We examined the specimens for the presence of astrocytic hyperplasia, inflammatory cells, edema, and gliosis. Histopathological changes were scored from 0 to 3, based on the presence and extent of neuritic plaques, neurofibrillary tangles, and beta-amyloid deposition (Hyman et al., 2012).

ELISA of Brain Acetylcholine

The protein level of ACh (nmol/mg tissue protein) was calculated according to the manufacturer's brochure (MyBiosource, San Diego, CA, USA).

Catalytic Activity of Acetylcholinesterase

The catalytic activity of AChE (units/L) was assessed by the thiocholine production rate using spectrophotometry (Jenway, USA). Fifty μL of rats' brain tissue homogenate was added to the assay buffer and the working reagent as per the manufacturer's recommendations (Sigma-Aldrich). Absorption was determined at 412 nm for a period of 10 minutes at 2-minute intervals.

Quantitative Real-Time Polymerase Chain Reaction of Brain Homogenate

The gene expressions of *AChE*, *MT2*, *D5*, *ANGPTL4*, and *KLF9* were detected using the RNeasy Purification Reagent (Promega, Madison, WI, USA). Spectrophotometry (Jenway) was used to measure the isolated RNA at 260 nm. The extracted RNA was reverse transcribed into cDNA by a Reverse Transcription System Kit (Fermentas, USA). The cDNA was produced from 5 μg of total RNA extracted with 1 μL (20 pmol) of antisense primer and 0.8 μL of superscript AMV reverse transcriptase for 60 minutes at 37°C. The relative abundances of the mRNA species were assessed by the SYBR Green method and an ABI Prism7500 Sequence Detector System Applied Biosystem with software version 3.1 (StepOne, USA). The PCR primers used were designed with Gene Runner Software (Hastings Software Inc., Hastings, NY, USA) from RNA sequences in GenBank (Table 1). All primer sets had a calculated annealing temperature of 60°C. Quantitative reverse-transcription polymerase chain reaction analysis was performed in duplicate in a 25-μL reaction volume consisting of 2× SYBR Green PCR Master Mix (Applied Biosystems, USA), 900 nM of each primer, and 2 to 3 μL of cDNA. The amplification conditions were 2 minutes at 50°C, 10 minutes at 95°C, and 40 cycles of denaturation at 95°C for 15 seconds and annealing/extension at 60°C for 10 minutes. Data from the real-time assays were calculated by Sequence Detection Software version 1.7 (PE Biosystems, Foster City, CA, USA). The relative expression levels of AChE, MT2, D5, ANGPTL4, and KLF9 were calculated by the comparative Ct method as stated by the manufacturer's recommendations (Applied Biosystems, USA). Normalization for variation in the expression of each target gene was performed in reference to the mean critical threshold values of glyceraldehyde 3-phosphate dehydrogenase (GAPDH) housekeeping gene expression by the $\Delta\Delta$Ct method.

Statistical Analysis

Sample size calculation was done using G*Power software v. 3.1.9.4., at a level of significance alpha = 0.05 and power (1-beta) = 0.9. Data were coded and entered using the Statistical Package for the Social Sciences v. 28 (IBM Corp., Armonk, NY, USA). Normally distributed quantitative variables were presented as mean ± S.D. Nonnormally distributed quantitative variables were presented as median and interquartile range. Comparisons between groups were done using ANOVA with multiple comparisons post hoc Tukey's test for the normally distributed quantitative variables. The Kruskal–Wallis test with multiple comparisons post hoc adjusted Mann–Whitney test were used for the nonnormally distributed quantitative variables. Correlations between quantitative variables were done using Spearman *rho* correlation coefficient. A P value < 0.05 was considered statistically significant.

Results

When comparing the behavioral, electrophysiological, biochemical, and pathologic aspects, no significant differences

TABLE 1
Primers Sequences of *AChE*, *MT2*, *D5*, *ANGPTL4*, *KLF9*, and *GAPDH* as housekeeping genes

Parameter	Forward and Reverse Primers	Gene Bank Accession Number
AChE	Forward: 5′-TTGGAGTCTCGAGGGTCATT-3′ Reverse: 5′-GGACGAGGGCTCCTACTTTC-3′	XM_039089843.1
MT2	Forward: 5′-CCCCACAGCCTCTTCTTAGCACTTG-3′ Reverse: 5′-CAGATGCACCAGTAGCGGTTGATG-3′	NM_001393841.1
D5	Forward: 5′-CCACATGATACCGAATGCAG-3′ Reverse: 5′-CACAGTCAAGCTCCCAGACA-3′	NM_012768.1
ANGPTL4	Forward: 5′-CCAATGGCCTTTCCCTGCCCTT-3′ Reverse: 5′-TTTTACGCTGCTGCCGTTGCC-3′	XM_039079419.1
KLF9	Forward: 5′-AAGCTCCGCAGCCACCCTCA-3′ Reverse: 5′-CGGCGCGGTTGGAGATGGAA-3′	>NM_057211.2
GAPDH (House keeping)	Forward primer: 5′-GATGCTGGTGCTGAGTATGTCG-3′ Reverse primer: 5′-GTGGTGCAGGATGCATTGCTGA-3′	NM_017008.4

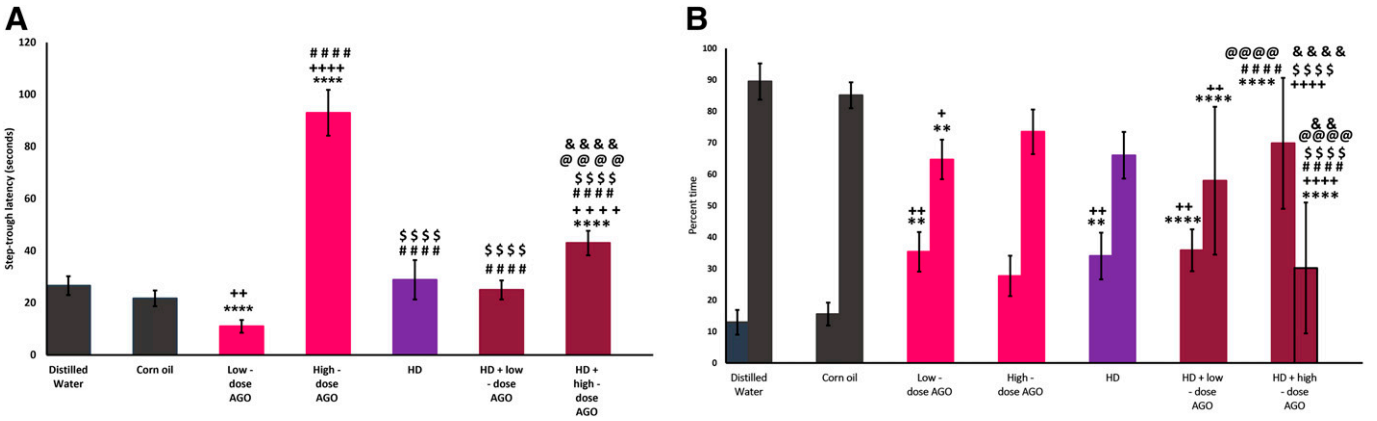

Fig. 2. Dim to bright light preference test. Adult male Wistar albino rats subdivided into control (oral DW or i.p. corn oil), low-dose AGO (oral 40 mg/kg), high-dose AGO (oral 80 mg/kg), HD (i.p. 4 mg/kg, once weekly), HD + low-dose AGO, and HD + high-dose AGO, showing (A) step-through latency (seconds) until the rats enter the dim partition with all four paws; (B) the percent time spent in the bright light (right column bars) and dim compartments (left column bars). Data are expressed as mean ± S.D. Significant when $P < 0.05$. $^{**}P < 0.01$, $^{****}P < 0.0001$ compared with controls (DW). $^{+}P < 0.05$, $^{++}P < 0.01$, $^{++++}P < 0.0001$ compared with controls (corn oil). $^{\#\#\#\#}P < 0.0001$ compared with low-dose AGO. $^{\$\$\$\$}P < 0.0001$ compared with high-dose AGO. $^{@@@@}P < 0.0001$ compared with HD. $^{\&\&}P < 0.01$, $^{\&\&\&\&}P < 0.0001$ compared with HD + low-dose AGO. Low-dose AGO: 40 mg/kg; high-dose AGO: 80 mg/kg.

were identified between control rats receiving corn oil and those administered DW. The comparison with controls was applied to both receiving DW or corn oil, but ρ values mentioned in the text involved comparison relative to control rats receiving DW, unless indicated otherwise.

HD + High-Dose AGO Ameliorated the Indices of Dim-to-Bright Light Preference and Y-Maze Tests

HD + High-Dose AGO Prolonged the Step-through Latency. Compared with controls, 6-week administration of daily oral low-dose AGO reduced the step-through latency (seconds) by –58.69% [$F(6, 49) = 206.348$, $P < 0.0001$] (Fig. 2A), while it increased the percent time spent in bright light by +173.03% [$F(6, 49) = 30.636$, $P < 0.0001$], against reducing the percent time spent in dim light by –27.70% [$F(6, 49) = 18.321$, $P = 0.007$] (Fig. 2B).

Unlike the low-dose, high-dose AGO prolonged the step-through latency relative to controls by +249.23% [$F(6, 49) = 206.348$, $P < 0.0001$] (Fig. 2A), without affecting the percent time spent in bright or that spent in dim light (Fig. 2B).

When testing the short-term memory and spatial memory of adult male rats, long-term weekly injections of HD resulted in significantly higher percent time spent in bright light compared with controls (+162.75%) [$F(6, 49) = 30.636$, $P = 0.001$] without affecting the percent time spent in dim light or the step-through latency, relative to controls (Fig. 2, A and B).

When compared with controls, HD + low-dose AGO did not affect the step-through latency (Fig. 2A) but increased the percent time spent in bright light by +176.82% [$F(6, 49) = 30.636$, $P < 0.0001$], as was with either treatment, against reducing the percent time spent in dim light by –35.23% [$F(6, 49) = 18.321$, $P < 0.0001$] (Fig. 2B).

HD + high-dose AGO prolonged the step-through latency relative to controls by +61.47% [$F(6, 49) = 206.348$, $P < 0.0001$] (Fig. 2A), together with increasing the percent time spent in bright light by +439.49% [$F(6, 49) = 30.636$, $P < 0.0001$], versus reducing the percent time spent in dim light by –66.25% [$F(6, 49) = 18.321$, $P < 0.0001$] (Fig. 2B).

HD + High-Dose AGO Increased the Percent of Alternations. Compared with controls, no significant changes were noticed in the other studied groups regarding the number of alternations in the Y maze paradigm (Fig. 3A).

While both low and high AGO doses reduced the percent of alternations between the arms of the Y-maze relative to

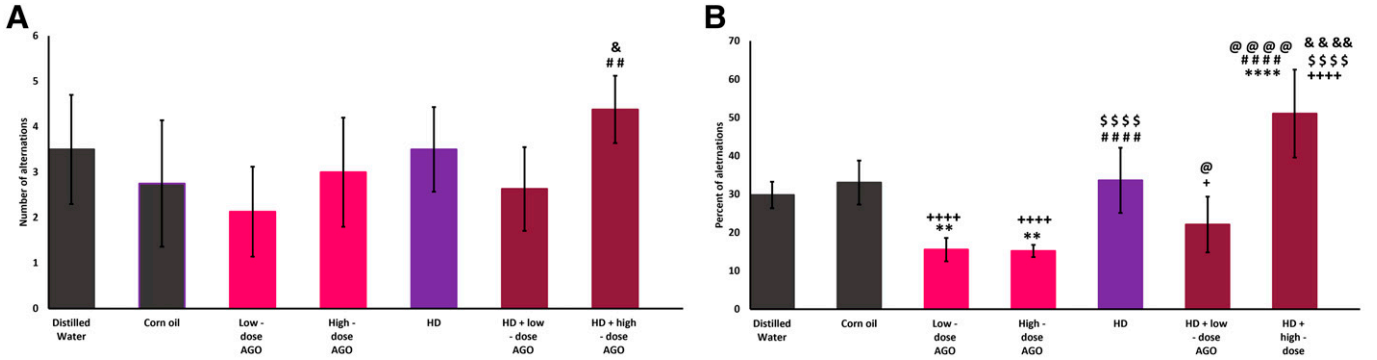

Fig. 3. Y-maze test. Adult male Wistar albino rats subdivided into control (oral DW or i.p. corn oil), low-dose AGO (oral 40 mg/kg), high-dose AGO (oral 80 mg/kg), HD (i.p. 4 mg/kg, once weekly), HD + low-dose AGO, and HD + high-dose AGO, showing (A) number of alternations; (B) percent of alternations. Data are expressed as mean ± S.D. Significant when $P < 0.05$. $^{**}P < 0.01$, $^{****}P < 0.0001$ compared with control group (DW). $^{+}P < 0.05$, $^{++++}P < 0.0001$ compared with controls (corn oil). $^{\#\#}P < 0.01$, $^{\#\#\#\#}P < 0.0001$ compared with low-dose AGO. $^{\$\$}P < 0.01$, $^{\$\$\$\$}P < 0.0001$ compared with high-dose AGO. $^{@}P < 0.05$, $^{@@@@}P < 0.0001$ compared with HD. $^{\&}P < 0.05$, $^{\&\&\&\&}P < 0.0001$ compared with HD + low-dose AGO. Low-dose AGO: 40 mg/kg; high-dose AGO: 80 mg/kg.

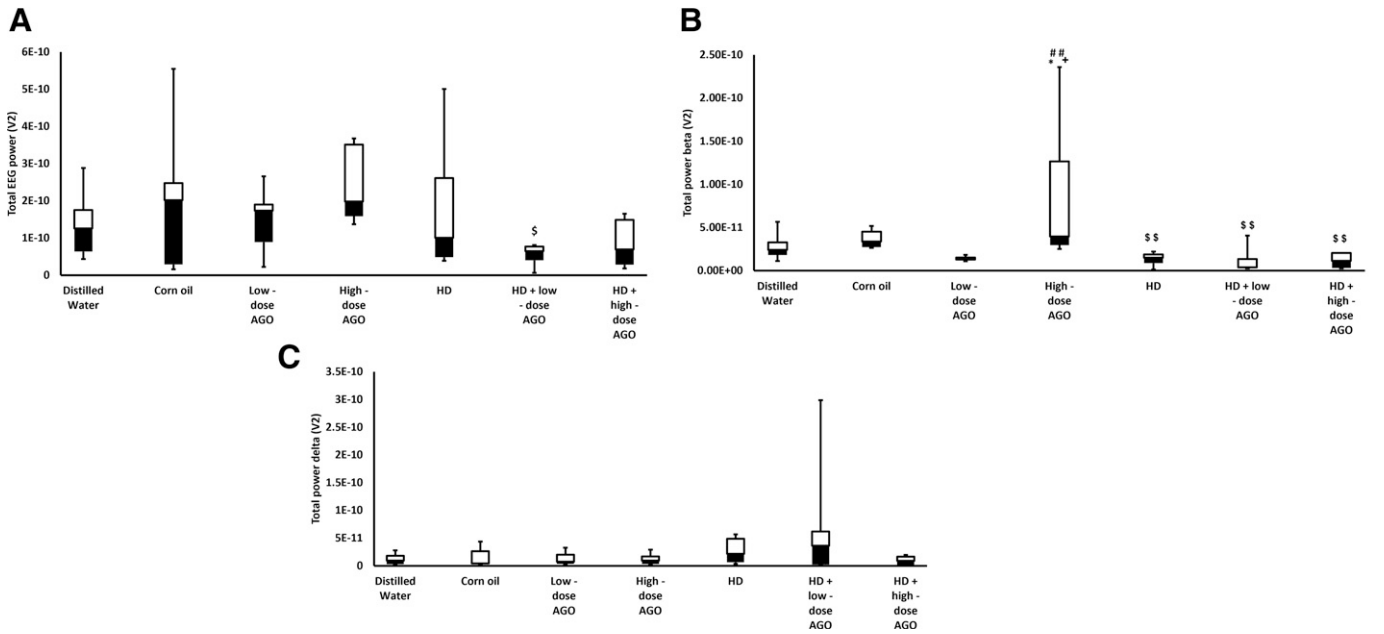

Fig. 4. Total EEG power (V^2) of adult male Wistar albino rats subdivided into control (oral DW or i.p. corn oil), low-dose AGO (oral 40 mg/kg), high-dose AGO (oral 80 mg/kg), HD (i.p. 4 mg/kg, once weekly), HD + low-dose AGO, and HD + high-dose AGO, showing (A) source wave; (B) beta wave; (C) delta wave. Data are expressed as median and interquartile range. Significant when $P < 0.05$. $^{*}P < 0.05$ compared with control (DW). $^{+}P < 0.05$ compared with controls (corn oil). $^{\#\#}P < 0.01$ compared with low-dose AGO. $^{\$}P < 0.05$, $^{\$\$}P < 0.01$ compared with high-dose AGO. Low-dose AGO: 40 mg/kg; high-dose AGO: 80 mg/kg.

controls by –47.74% and –48.94%, respectively [F (6, 49) = 28.046, $P = 0.002$ and $P < 0.001$], HD did not affect such a paradigm (Fig. 3B).

Comparing HD + low-dose AGO to controls receiving DW, there was no significant change regarding the percent of alternations. However, relative to controls receiving corn oil, the percent of alternations was reduced by –33.10% [F(6, 49) = 28.046, $P = 0.030$] (Fig. 3B).

Notably, HD + high-dose AGO increased the percent of alternations relative to controls by +71.25% [F(6, 49) = 28.046, $P < 0.0001$] (Fig. 3B).

HD + High-Dose AGO Reduced the Mean Power Frequency of Source and Beta EEG Waves

HD + High-Dose AGO Redeemed the Total Beta Power to Control Level. In all studied groups, total EEG power (V^2) was not significantly affected (Fig. 4A).

Neither low-dose AGO nor HD affected total beta power; however, high-dose AGO increased total beta power (V^2) relative to controls by +206.00% [t (6) = 28.670, $P = 0.014$] (Figs. 4B and 7A).

Combined HD + low-dose AGO did not affect total beta power, consistent with the effect of either medication in this context (Figs. 4B and 7A). Combined HD + high-dose AGO redeemed the total beta power to the control level (Figs. 4B and 7A). The total delta power (V^2) was not affected in any of the studied groups (Fig. 4C), as was with total EEG power.

HD + High-Dose AGO Reduced the Mean Power Frequency of Source EEG Wave. While the mean power frequency of the source wave (Hz) was increased with HD relative to controls by +32.54% [F(6, 49) = 12.400, $P = 0.001$] (Figs. 5A and 7B), neither low-nor high-dose AGO affected the mean power frequency of the source wave (Fig. 5A).

Combined HD + low-dose AGO redeemed the mean power frequency of the source wave to the control level, in contrast to HD + high-dose AGO, which reduced the mean power frequency of the source wave by –23.39% [F (6, 49) = 12.400, $P = 0.044$] (Figs. 5A and 7B).

As for the mean power frequency beta (Hz), it was not significantly different when comparing the treated groups to controls receiving DW. However, when compared with controls receiving corn oil, the mean power frequency beta was reduced with both low and high AGO doses by –35.92% and –39.07%, respectively [F(6, 49) = 9.389, $P < 0.0001$] as well as with HD by –36.42% [F (6, 49) = 9.389, $P < 0.0001$] (Figs. 5B and 7C).

Consistent with the effect of either medication, combined HD + AGO, regardless of the AGO dose, displayed reduced mean power frequency beta relative to controls receiving corn oil by –35.12% and –37.12%, respectively [F (6, 49) = 9.389, $P < 0.0001$], but such differences did not reach significance when compared with controls receiving DW (Figs. 5B and 7C).

While the mean power frequency delta (Hz) with low-dose AGO was reduced relative to controls by –38.01% [F (6, 49) = 2.207, $P = 0.037$], neither high-dose AGO nor HD affected the mean power frequency delta (Fig. 5C).

Combined HD + low-dose AGO redeemed the mean power frequency delta, while HD + high-dose AGO did not affect it, as was with either treatment (Fig. 5C).

HD + High-Dose AGO Redeemed the Mean Amplitudes of Source, Beta, and Delta Waves. While low-dose AGO did not affect the mean amplitude of the source wave (μV), both high-dose AGO and HD increased the mean amplitude of the source wave relative to controls by +278.17% and +105.65%, respectively [t (6) = 45.706, $P < 0.0001$] (Figs. 6A and 7D).

While HD + low-dose AGO exhibited a persistently higher mean amplitude of source wave relative to controls (+189.16%)

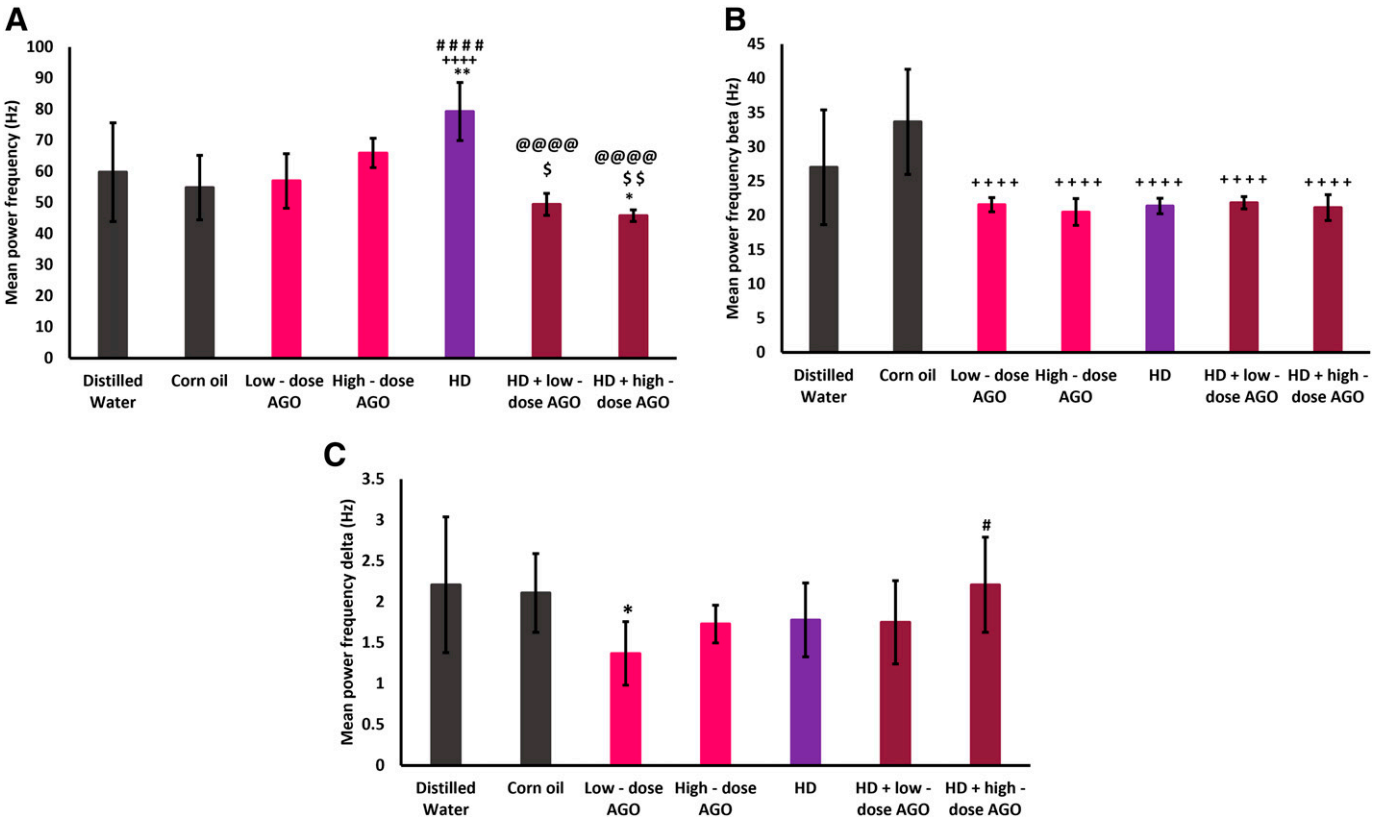

Fig. 5. Mean power frequency (Hz) of adult male Wistar albino rats subdivided into control (oral DW or i.p. corn oil), low-dose AGO (oral 40 mg/kg), high-dose AGO (oral 80 mg/kg), HD (i.p. 4 mg/kg, once weekly), HD + low-dose AGO, and HD + high-dose AGO, showing (A) source wave; (B) beta wave; (C) delta wave. Data are expressed as mean ± S.D. Significant when $P < 0.05$. $^{*}P < 0.05$, $^{**}P < 0.01$ compared with controls (DW). $^{++++}P < 0.0001$ compared with controls (corn oil). $^{\#}P < 0.05$, $^{\#\#\#\#}P < 0.0001$ compared with low-dose AGO. $^{\$}P < 0.05$, $^{\$\$}P < 0.01$ compared with high-dose AGO. $^{@@@@}P < 0.0001$ compared with HD. Low-dose AGO: 40 mg/kg; high-dose AGO: 80 mg/kg.

[t (6) = 45.706, $P < 0.0001$], HD + high-dose AGO redeemed the mean amplitude of the source wave to that of control rats (Figs. 6A and 7D).

Moreover, with both high-dose AGO and HD, the predominance of positive source waves was observed, unlike controls displaying, mainly, negative EEG waves (Figs. 6A and 7D).

The predominance of negative source waves was restored with combined treatment, regardless of the AGO dose, as was with controls (Figs. 6A and 7D).

High-dose AGO increased the mean beta amplitude (μV) relative to controls by +414.29% [t (6) = 45.116, $P < 0.0001$] (Figs. 6B and 7E), an effect that was not observed with either low-dose AGO or HD, alone or combined.

Notably, the high-dose AGO-mediated beta amplitude increase was redeemed to control levels with HD + high-dose AGO (Fig. 6B).

Concerning beta polarity, low-dose AGO displayed predominantly negative beta waves, thus reverting the positive polarity of beta wave in controls (Fig. 6B). Both high-dose AGO and HD, whether alone or combined, exhibited similar positive polarity as in controls (Fig. 6B). The negative polarity of beta wave persisted with combined HD + low-dose AGO (Fig. 6B).

Regarding the mean delta amplitude (μV), while low-dose AGO did not affect it, both high-dose AGO and HD exhibited higher mean delta amplitudes relative to controls by +167.27% and +265.00%, respectively [t(6) = 41.331, $P < 0.0001$] (Figs. 6C and 7F).

Notably, increased mean delta amplitude persisted with combined HD + low-dose AGO (+330.46%) [t(6) = 45.116, $P < 0.0001$]. Conversely, combined HD + high-dose AGO redeemed the mean delta amplitude to that of controls (Figs. 6C and 7F).

Moreover, the predominance of positive delta wave was obvious with both high-dose AGO and HD, unlike the predominantly negative delta wave seen with controls (Fig. 6C). While the predominance of positive polarity persisted with combined HD + low-dose AGO, combined HD + high-dose AGO redeemed delta polarity to negative as in controls (Figs. 6C and 7F).

In ECG Recordings HD + High-Dose Prolonged RR Interval, in Association with Tall R and Inverted P and T Waves

HD + High-Dose Redeemed the Heart Rate to Control Level. Noticeably, as compared with control rats, the heart rate (bpm) was reduced with both high-dose AGO and HD by –21.75% [F(6, 49) = 7.821, $P < 0.012$] and –26.20% [F (6, 49) = 7.821, $P = 0.001$], respectively. Meanwhile, the heart rate was not affected with low-dose AGO (Fig. 8A).

With combination therapy, regardless of the AGO dose, the heart rate was redeemed to that of controls (Fig. 8A).

HD + High-Dose AGO Exhibited an Inverted P, with Shortening of P Wave Duration. In comparison with controls, both high-dose AGO and HD reduced the P wave amplitude (millivolts) by –54.13% [F (6, 49) = 11.392, $P = 0.001$] and –76.95% [F (6, 49) = 11.392, $P < 0.0001$], respectively,

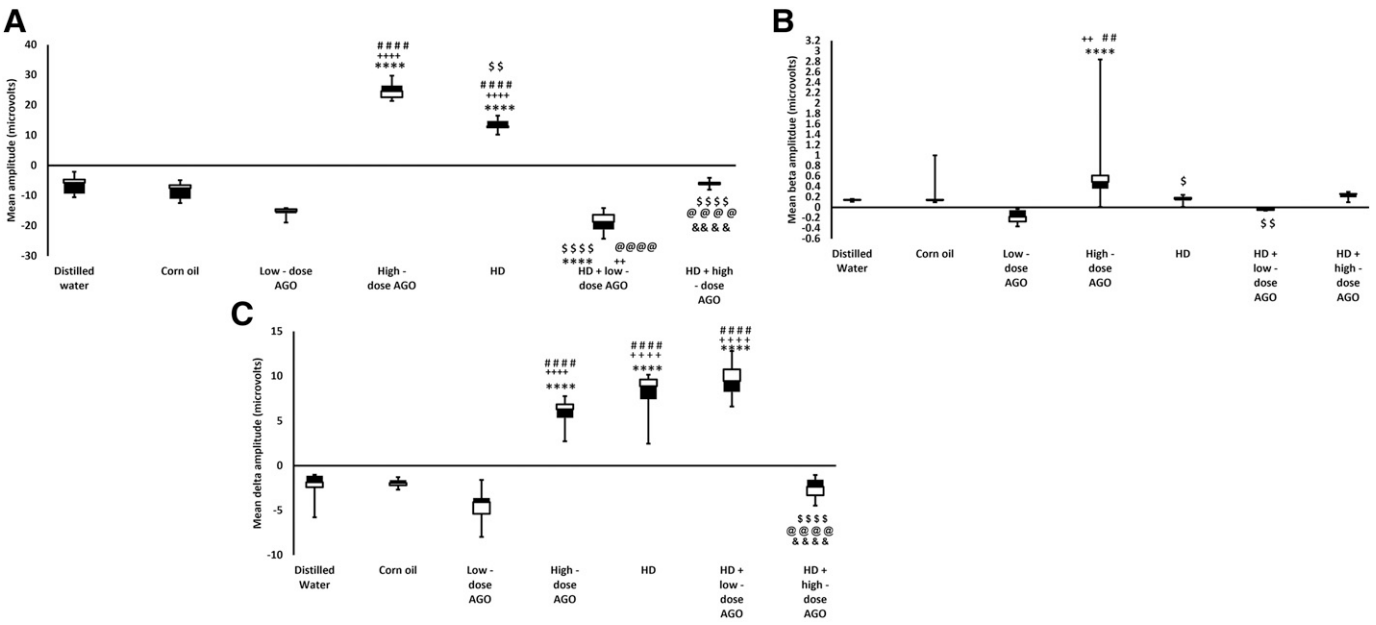

Fig. 6. Mean amplitude (microvolts) of adult male Wistar albino rats subdivided into control (oral DW or i.p. corn oil), low-dose AGO (oral 40 mg/kg), high-dose AGO (oral 80 mg/kg), HD (i.p. 4 mg/kg, once weekly), HD + low-dose AGO, and HD + high-dose AGO, showing (A) source wave; (B) beta wave; (C) delta wave. Data are expressed as median and interquartile range. Significant when $P < 0.05$. $^{****}P < 0.0001$ compared with controls (DW). $^{++}P < 0.01$ compared with controls (corn oil). $^{++++}P < 0.0001$ compared with controls (corn oil). $^{\#\#}P < 0.01$, $^{\#\#\#\#}P < 0.0001$ compared with low-dose AGO. $^{\$}P < 0.05$, $^{\$\$}P < 0.01$, $^{\$\$\$\$}P < 0.0001$ compared with high-dose AGO. $^{@@@@}P < 0.0001$ compared with HD. $^{\&\&\&\&}P < 0.0001$ compared with HD + low-dose AGO. Low-dose AGO: 40 mg/kg; high-dose AGO: 80 mg/kg.

and reduced the P wave duration (milliseconds) by –27.64% and –36.53%, respectively [$F(6, 49) = 47.413$, $P < 0.0001$], while low-dose AGO reduced the P wave duration by –40.00% [$F(6, 49) = 47.413$, $P < 0.0001$] but did not affect the P wave amplitude (Fig. 8, B and C). Moreover, P was inverted with HD (Fig. 8B).

Combined HD + low-dose AGO did not redeem either the P wave amplitude or duration, to remain persistently reduced relative to controls by –64.80% [$F(6, 49) = 11.392$, $P < 0.0001$] and –25.03% [$F(6, 49) = 47.413$, $P < 0.0001$], respectively (Fig. 8, B and C). P was inverted as well (Fig. 8B).

In contrast, combined HD + high-dose AGO redeemed the P wave amplitude to control levels, but it was persistently inverted and of reduced duration relative to controls by –36.15% [$F(6, 49) = 47.413$, $P < 0.0001$] (Fig. 8, B and C).

HD + High-Dose AGO Reduced PR Interval. Notably, relative to controls, PR interval (milliseconds) was shorter with both AGO doses by –15.06% [$F(6, 49) = 17.210$, $P < 0.0001$] and –12.03% [$F(6, 49) = 17.210$, $P = 0.001$], respectively, as well as with HD (–16.14%) [$F(6, 49) = 17.210$, $P < 0.0001$] (Fig. 8D).

PR interval was redeemed to control levels with HD + low-dose AGO (Fig. 8D). However, HD + high-dose AGO exhibited a persistently reduced PR interval relative to controls by –19.91% [$F(6, 49) = 17.210$, $P < 0.0001$] (Fig. 8D).

HD + High-Dose Exhibited the Tallest R Wave. Both AGO doses as well as HD increased R wave amplitude (millivolts) relative to controls by +80.53% [$t(6) = 50.104$, $P = 0.003$], +131.09% [$t(6) = 50.104$, $P < 0.0001$], and +163.29% [$t(6) = 50.104$, $P < 0.0001$], respectively (Fig. 8E).

Relative to controls, tall R wave was also displayed with combination therapy, more obviously with HD + high-dose AGO, where it increased by +226.19% and +523.15%, respectively [$t(6) = 50.104$, $P < 0.0001$] (Fig. 8E).

HD + High-Dose Redeemed S Wave Amplitude to Control Level. While low-dose AGO reduced S wave amplitude (millivolts) relative to controls by –54.34% [$t(6) = 39.890$, $P = 0.002$], high-dose AGO did not affect S wave amplitude. Such S wave amplitude reduction was also evident with HD (–73.55%) [$t(6) = 39.890$, $P < 0.0001$] (Fig. 8F).

While HD + low-dose AGO displayed a persistently reduced S wave amplitude relative to controls by –95.26% [$t(6) = 39.890$, $P < 0.0001$], HD + high-dose AGO redeemed S wave amplitude to control levels (Fig. 8F).

The downward deflection of S wave amplitude was obvious with all studied groups, apart from HD + low-dose AGO, in which the S wave was directed upwards (Fig. 8F).

HD + High–Dose AGO Did Not Affect QRS Duration. Only low-dose AGO reduced QRS interval (milliseconds) relative to controls by –26.27% [$F(6, 49) = 8.680$, $P = 0.013$] (Fig. 8G).

Despite being unvaried from controls, HD exhibited a more prolonged QRS compared with high-dose AGO by +33.99% [$F(6, 49) = 8.680$, $P = 0.003$] (Fig. 8G). HD + low-dose AGO redeemed QRS interval to control levels. HD + high-dose AGO did not affect QRS interval, consistent with either drug (Fig. 8G).

HD + High-Dose AGO Redeemed QTc Interval to Control Level. Relative to controls, both AGO doses exhibited shorter QT interval (milliseconds) by –37.78% and –36.85%, respectively [$F(6, 49) = 22.284$, $P < 0.0001$] and QTc intervals (milliseconds) by –35.20% and –37.63%, respectively [$F(6, 49) = 48.047$, $P < 0.0001$], while with HD, QTc, but not QT interval, was reduced by –11.19% [$F(6, 49) = 48.047$, $P = 0.022$] (Fig. 8H).

QTc, but not QT interval, was persistently reduced with HD + low-dose AGO when compared with controls by –24.98% [$F(6, 49) = 48.047$, $P < 0.0001$], unlike the redeemed QT and QTc intervals with HD + high-dose AGO (Fig. 8H).

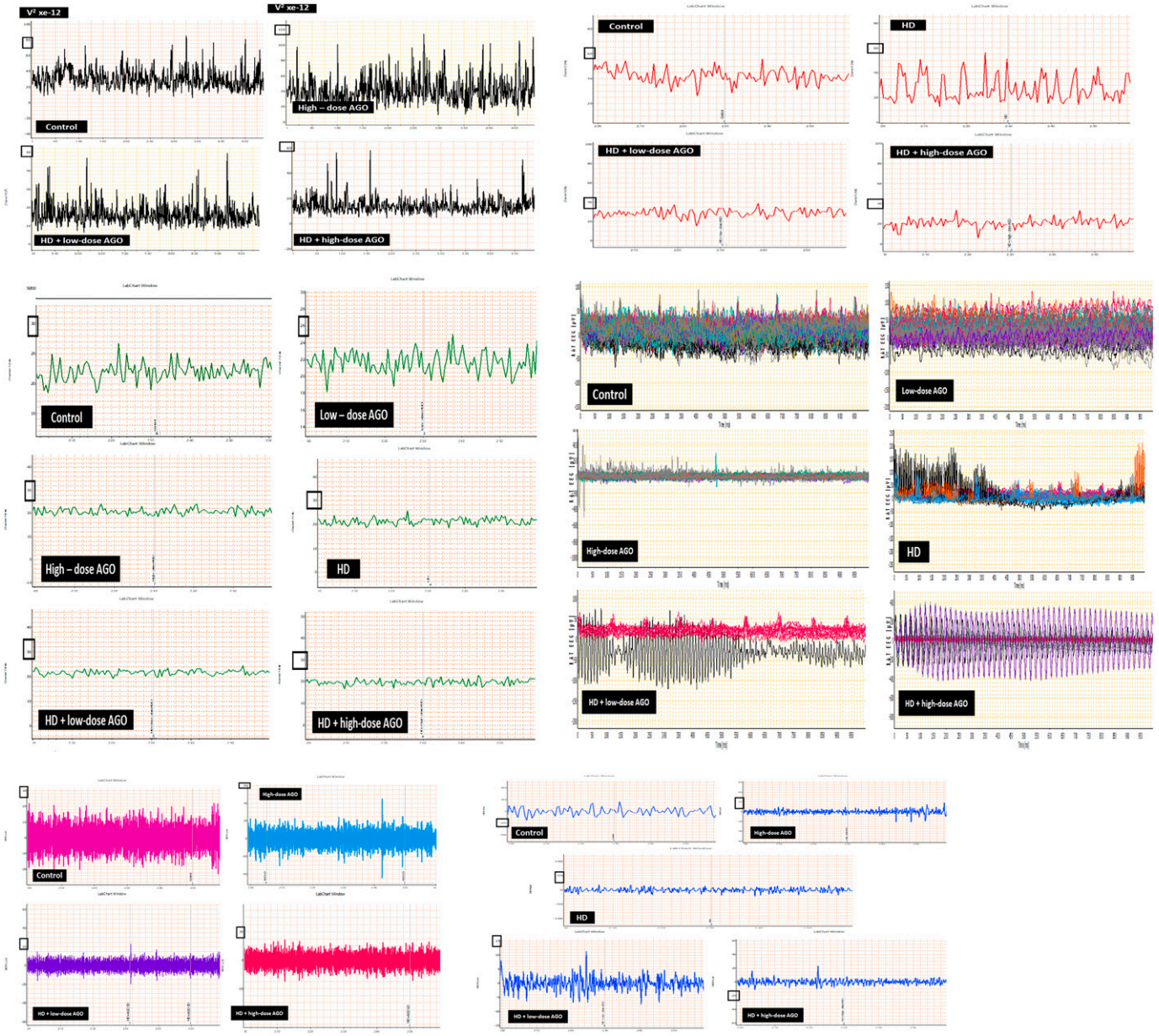

Fig. 7. Actual EEG tracings (PowerLab 4/30; ML866, ADInstruments, Australia) of adult male Wistar albino rats subdivided into control (oral DW or i.p. corn oil), low-dose AGO (oral 40 mg/kg), high-dose AGO (oral 80 mg/kg), HD (i.p. 4 mg/kg, once weekly), HD + low-dose AGO, and HD + high-dose AGO, showing (A) total beta power (V^2*E^{-12}); (B) mean power frequency source wave (Hz); (C) mean power frequency beta (Hz); (D) mean EEG amplitude (microvolts); (E) mean beta amplitude (microvolts); (F) mean delta amplitude (microvolts). Total power, mean power frequency, and mean amplitude are obtained by offline analysis of source, beta, and delta waves using LabChart v.7.2 software.

HD + High-Dose AGO Redeemed JT Interval. Both AGO doses as well as HD exhibited shorter JT intervals (milliseconds) relative to controls by –44.69% [F (6, 49) = 22.244, $P < 0.0001$], –56.63% [F (6, 49) = 22.244, $P < 0.0001$], and [F (6, 49) = 22.244, $P = 0.018$], respectively (Fig. 8I).

Combined HD + AGO, regardless of the AGO dose, redeemed JT interval to that of control rats (Fig. 8I).

HD + High-Dose AGO Exhibited ST Depression of High Amplitude. The amplitude of elevated ST (millivolts) seen with low-dose AGO exceeded the amplitudes of depressed ST seen with both controls by +717.26% [t(6) = 28.187, $P < 0.028$] and high-dose AGO by +1565.68% [t (6) = 28.187, $P < 0.044$] (Fig. 8J).

Although HD did not affect ST amplitude, it triggered ST elevation of an amplitude comparable to the ST depression seen with controls and high-dose AGO (Fig. 8J). Despite that combined HD + low-dose AGO redeemed the ST amplitude to control levels, ST was still elevated, unlike the ST depression in controls (Fig. 8J). Combined HD + high-dose AGO exhibited a depressed ST segment as controls but of amplitude exceeding controls by +1632.64% [t (6) = 28.187, $P < 0.0001$] (Fig. 8J).

HD + High-Dose AGO Displayed Inverted T Wave of Increased Amplitude. Neither AGO nor HD affected T wave amplitude (millivolts) when compared with controls (Fig. 8K). Similarly, combined HD + low-dose AGO did not affect T wave amplitude (Fig. 8K).

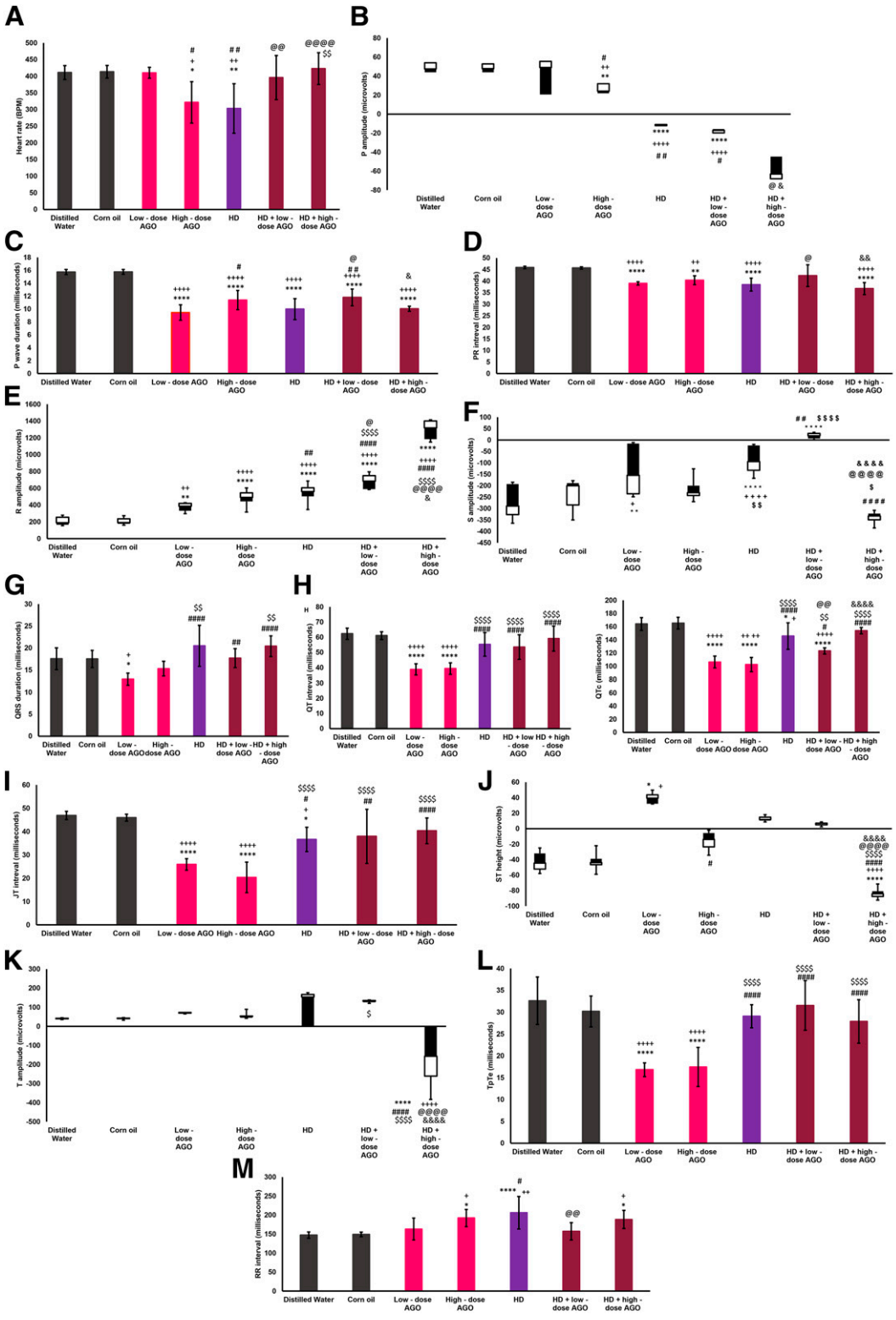

Fig. 8. ECG analysis of adult male Wistar albino rats subdivided into control (oral DW or i.p. corn oil), low-dose AGO (oral 40 mg/kg), high-dose AGO (oral 80 mg/kg), HD (i.p. 4 mg/kg, once weekly), HD + low-dose AGO, and HD + high-dose AGO, showing (A) heart rate (bpm). Data are expressed as mean ± S.D. (B) P wave amplitude (microvolts). Data are expressed as median and interquartile range. (C) P wave duration (milliseconds). Data are expressed as mean ± S.D. (D) PR interval (milliseconds). Data are expressed as mean ± S.D. (E) R wave amplitude (microvolts). Data are expressed as median and interquartile range. (F) S wave amplitude (microvolts). Data are expressed as median and interquartile range. (G) QRS duration (milliseconds). Data are expressed as mean ± S.D. (H) QT and QTc intervals (milliseconds). Data are expressed as mean ± S.D. (I) JT interval (milliseconds). Data are expressed as mean ± S.D. (J) ST amplitude (microvolts). Data are expressed as median and interquartile range. (K) T wave amplitude (microvolts). Data are expressed as median and interquartile range. (L) TpTe (milliseconds). Data are expressed as mean ± S.D. (M) RR interval (milliseconds). Data are expressed as mean ± S.D. Significant when $P < 0.05$. $^{*}P < 0.05$, $^{**}P < 0.01$, $^{****}P < 0.0001$ compared with controls (DW). $^{+}P < 0.05$, $^{++}P < 0.01$, $^{++++}P < 0.0001$ compared with controls (corn oil). $^{\#}P < 0.05$, $^{\#\#}P < 0.01$, $^{\#\#\#\#}P < 0.0001$ compared with low-dose AGO. $^{\$}P < 0.05$, $^{\$\$}P < 0.01$, $^{\$\$\$\$}P < 0.0001$ compared with high-dose AGO. $^{@}P < 0.05$, $^{@@}P < 0.01$, $^{@@@@}P < 0.0001$ compared with HD. $^{\&}P < 0.05$, $^{\&\&}P < 0.01$, $^{\&\&\&\&}P < 0.0001$ compared with HD + low-dose AGO.

Combined HD + high-dose AGO exhibited a higher T wave amplitude relative to controls by +303.47% [$t(6) = 34.150$, $P < 0.0001$]. Also, T wave was inverted with HD + high-dose AGO, unlike controls and the other studied groups (Fig. 8K).

HD + High-Dose AGO Redeemed T Peak-Tend Interval to Control Level. Both AGO doses reduced TpTe interval (milliseconds) relative to controls by –48.42% and –46.49%, respectively [$F(6, 49) = 18.951$, $P < 0.0001$], while HD did not affect TpTe interval (Fig. 8L). Combined HD + AGO, regardless of the AGO dose, redeemed the TpTe interval to control level (Fig. 8L).

HD + High-Dose AGO Prolonged RR Interval. While low-dose AGO did not affect RR interval (milliseconds), both high-dose AGO and HD prolonged RR interval beyond control levels by +30.60% [$F(6, 49) = 7.034$, $P < 0.012$] and +40.01% [$F(6, 49) = 7.034$, $P < 0.0001$], respectively (Fig. 8M).

While combined HD + low-dose AGO redeemed RR to control levels, combined HD + high-dose AGO displayed a persistently prolonged RR interval relative to controls by +27.97% [$F(6, 49) = 7.034$, $P = 0.028$], consistent with the individual effects of HD and high-dose AGO (Fig. 8M). Actual ECG tracings illustrated some of the aforementioned differences among the studied groups (Fig. 9, A–F).

HD + High-Dose AGO Redeemed the Weights of Both Brain Hemispheres to Control Levels

HD + High-Dose AGO Did Not Affect Body Weight. Compared with controls, neither AGO nor HD affected the body weight of rats (Fig. 10A).

In contrast, combined HD + low-dose AGO increased the body weight of rats relative to controls by +20.36% [$F(6, 49) = 7.466$, $P = 0.002$] (Fig. 10A), while combined HD + high-dose AGO did not affect the rats' body weight, which was consistent with the effects of individual treatments (Fig. 10A).

HD + High-Dose AGO Redeemed the Weights of Both Right and Left Brain Hemispheres. Compared with controls, both AGO doses reduced the weight of each of the right brain hemisphere by –25.16% and –23.27%, respectively [$F(6, 49) = 72.087$, $P < 0.0001$] and left brain hemisphere by –20.81% and –13.42%, respectively [$F(6, 49) = 47.732$, $P < 0.0001$], more obvious with low-dose AGO, unlike HD which did not affect the weight of the brain hemispheres (Fig. 10, B and C).

Combination therapy with either AGO dose was able to resolve the changes seen with AGO monotherapy, redeeming the weights of the right and left brain hemispheres to control levels (Fig. 10, B and C).

HD + High-Dose AGO Ameliorated the Microstructural Changes Provoked by Either Drug

While control rats showed normal brain microstructure (Fig. 11A), prolonged low-dose AGO yielded mild fascicular edema of the brain, together with astrocytic hyperplasia and reactive gliosis, associated with scarce neuritic plaques (Fig. 11B), scored as A0, B1, and C1, based on the respective absence of beta-amyloid plaques, presence of scarce neurofibrillary tangles in limited areas, and infrequently encountered neuritic plaques.

High-dose AGO resulted in mild to moderate inflammatory cellular infiltrate of the brain with mild fascicular edema, accompanied by astrocytic hyperplasia, and reactive gliosis (Fig. 11C), scored as A0, B0, and C1, based on the respective

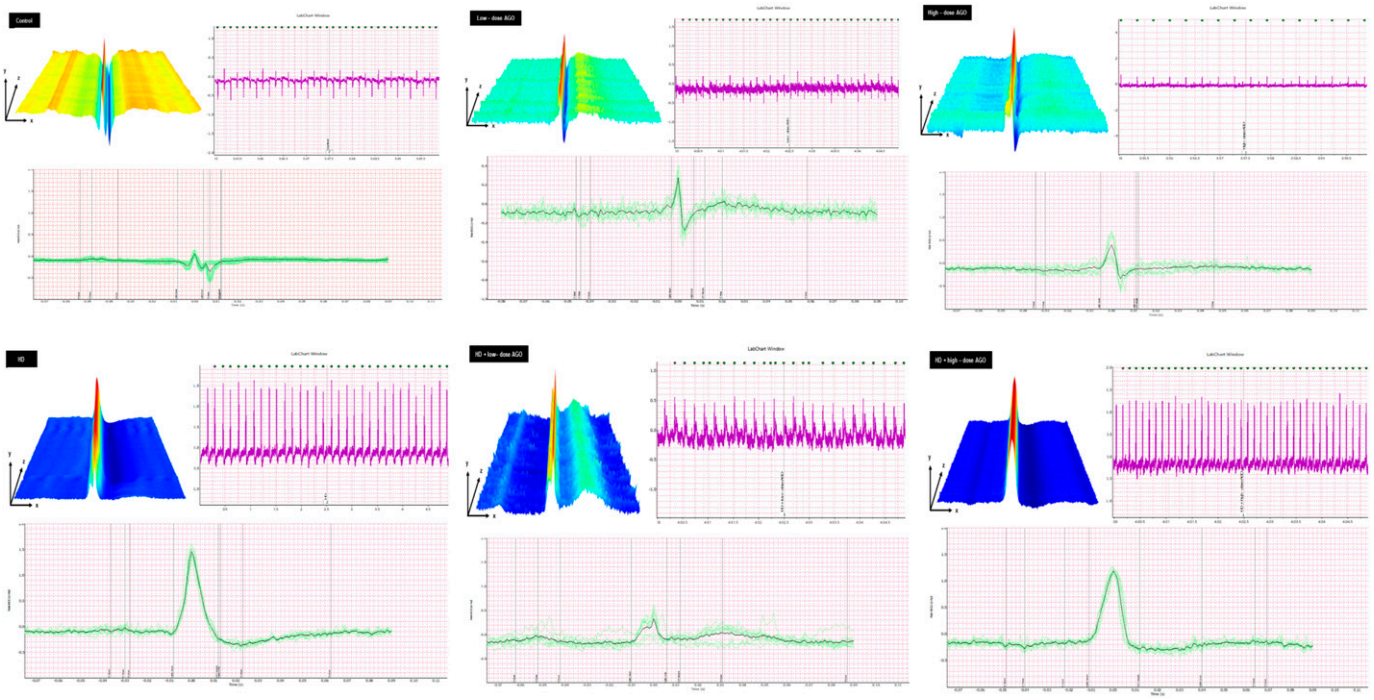

Fig. 9. Actual ECG tracing of (A) control group (receiving either DW or corn oil); (B) low-dose AGO (oral 40 mg/kg, daily); (C) high-dose AGO (oral 80 mg/kg, daily); (D) HD (i.p. 4 mg/kg, once weekly); (E) HD + low-dose AGO; (F) HD + high-dose AGO. Recordings are done using (PowerLab 4/30; ML866, ADInstruments, Australia), and tracings are generated using LabChart v.7.2 software. In each 9A to 9F: Upper left tracing: Waterfall plot depicting three-dimentional aspects of the stacked averaged successive heart betas recorded over 5 minutes, showing duration [horizontal plane (x-axis)], amplitude [vertical plane (y-axis)], along timing axis (z plane). Upper right tracing: ECG beats for 1 minute. Lower tracing: Averaging 10 beats.

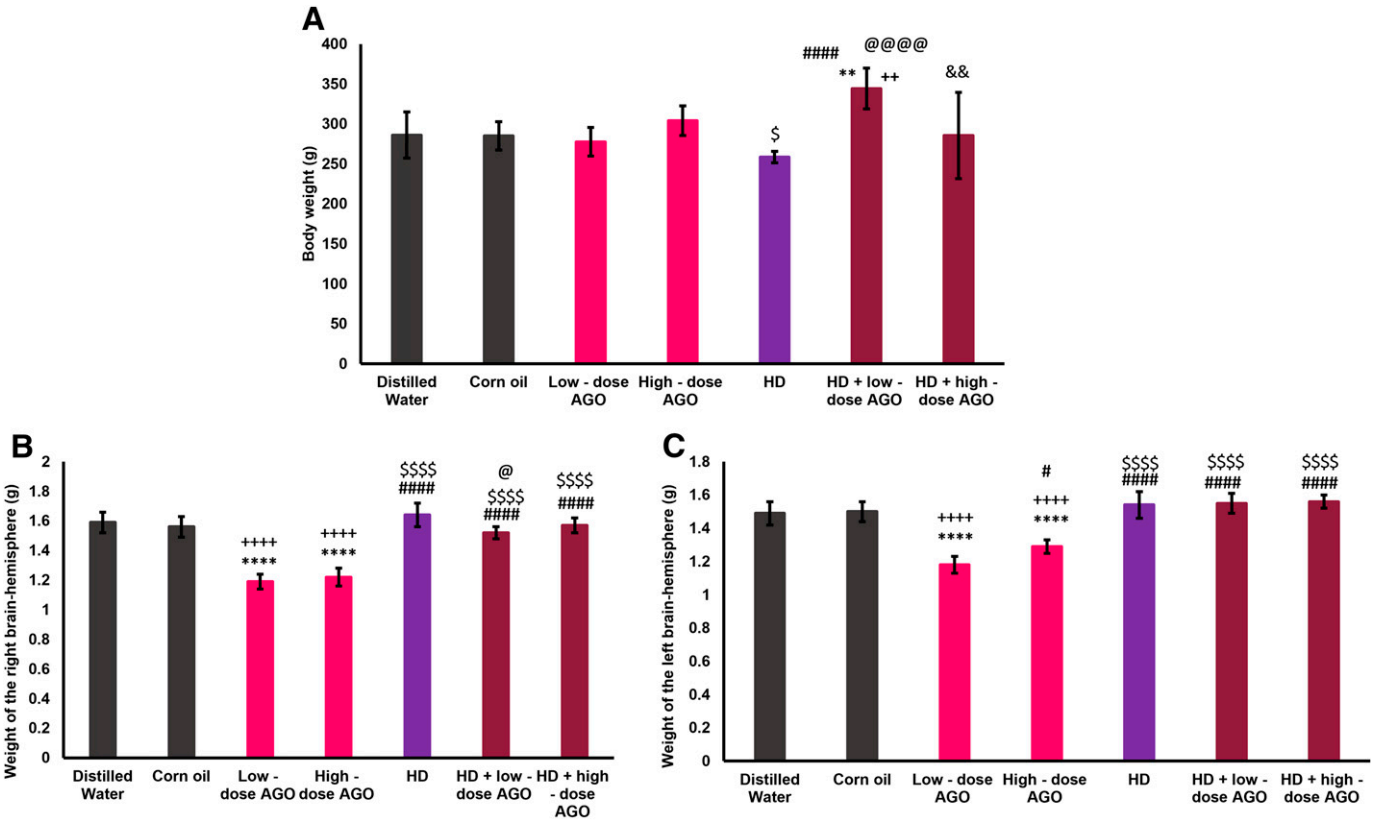

Fig. 10. Body and brain weights of adult male Wistar albino rats subdivided into control (oral DW or i.p. corn oil), low-dose AGO (oral 40 mg/kg), high-dose AGO (oral 80 mg/kg), HD (i.p. 4 mg/kg, once weekly), HD + low-dose AGO, and HD + high-dose AGO, showing (A) body weight; (B) weight of the right brain hemisphere; (C) weight of the left brain-hemisphere. Data are expressed as mean ± S.D. Significant when $P < 0.05$. $^{**}P < 0.01$, $^{****}P < 0.0001$ compared with controls (DW). $^{++}P < 0.01$, $^{++++}P < 0.0001$ compared with controls (corn oil). $^{\#}P < 0.05$, $^{\#\#\#\#}P < 0.0001$ compared with low-dose AGO. $^{\$}P < 0.05$, $^{\$\$\$\$}P < 0.0001$ compared with high-dose AGO. $^{@}P < 0.05$, $^{@@@@}P < 0.0001$ compared with HD. $^{\&\&}P < 0.01$ compared with HD + low-dose AGO.

absence of beta-amyloid plaques, neurofibrillary tangles, and infrequently encountered neuritic plaques.

Weekly HD injections for 6 weeks induced moderate fascicular edema, astrocytic hyperplasia, and reactive gliosis, added to scattered neurofibrillary tangles (Fig. 11D). Such changes were scored as A0, B1, and C2, based on the respective absence of beta-amyloid plaques, presence of neurofibrillary tangles in limited areas, and frequently encountered neuritic plaques.

Combined HD + low-dose AGO caused mild fascicular edema, with remaining astrocytic hyperplasia, reactive gliosis, scattered neurofibrillary tangles as well as few neuritic plaques (Fig. 11E) and had an average score of A0, B1, and C1, based on the respective absence of beta-amyloid plaques, presence of neurofibrillary tangles in limited areas, and infrequently encountered neuritic plaques.

Combined HD + high-dose AGO yielded mild fascicular edema with minimal astrocytic hyperplasia and reactive gliosis (Fig. 11F) and a score of A0, B0, and C0, based on the respective absence of beta-amyloid plaques, neurofibrillary tangles, and neuritic plaques.

HD+ High-Dose AGO Reduced Brain ACh Level and MT2 Expression, Against Increasing D5 Expression While Redeeming KLF9 to Control Levels

HD+ High-Dose AGO Reduced Brain ACh Level, with Redemption of Brain AChE Expression and Activity. In contrast to both AGO doses, which increased brain ACh relative to controls by +76% and +32%, respectively [F (6, 49) = 1441.982, $P < 0.0001$], HD reduced the brain level of ACh by –26% [F (6, 49) = 1441.982, $P < 0.0001$] (Fig. 12A).

Combined HD to either AGO dose ameliorated the variations in brain ACh level, as demonstrated by significantly higher ACh levels relative to HD [F (6, 49) = 1441.982, $P <$ 0.0001] and significantly lower ACh levels relative to AGO doses [F(6, 49) = 1441.982, $P < 0.0001$]. Such recovery was incomplete, so that HD + low-dose AGO and HD + high-dose AGO exhibited persistently reduced brain ACh levels relative to controls by –7.33% and –10.67%, respectively [F(6, 49) = 1441.982, $P < 0.0001$] (Fig. 12A).

Paradoxically, both AGO doses displayed increased brain AChE expression beyond control levels by +94.12% and +52.94%, respectively [F (6, 49) = 55.649, $P < 0.0001$] (Fig. 12B). This also applied to AChE activity, which was increased beyond the control level with both AGO doses by +29.55% and +23.52%, respectively [F(6, 49) = 151.60, $P < 0.0001$] (Fig. 12C). However, neither brain *AChE* expression nor activity was affected by prolonged HD treatment (Fig. 12, B and C).

While HD + low-dose AGO reduced brain AChE expression and activity relative to controls by –29.41% [F (6, 49) = 55.649, $P = 0.022$] and –26.93% [F (6, 49) = 151.60, $P = 0.018$], respectively, HD + high-dose AGO redeemed the brain AChE expression and activity to control levels (Fig. 12, B and C).

HD + High-Dose AGO Downregulated Brain MT2 Against Upregulating Brain D5. Aligned with the increased brain ACh and AChE observed with both AGO doses,

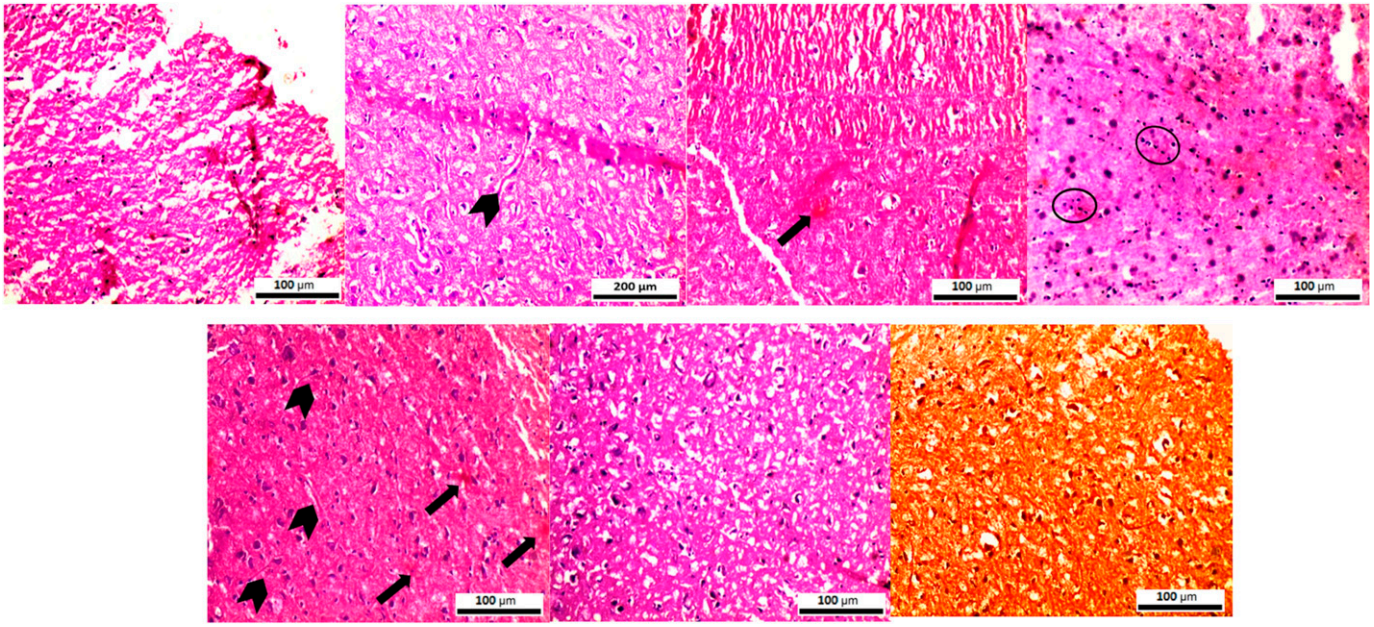

Fig. 11. H&E stained brain specimens of adult male Wistar albino rats subdivided into control (oral DW or i.p. corn oil), low-dose AGO (oral 40 mg/kg), high-dose AGO (oral 80 mg/kg), HD (i.p. 4 mg/kg, once weekly), HD + low-dose AGO, and HD + high-dose AGO, showing (A) normal brain tissue in control rats (H&E, 100x); (B) scattered neuritic plaques (arrow) with low-dose AGO (H&E, 100x); (C) mild to moderate inflammatory cellular infiltrate (circles) with high-dose AGO (H&E, 100x); (D) scattered neurofibrillary tangles (arrowhead) with HD (H&E, 200x); (E) scattered neurofibrillary tangles (arrowheads) as well as neuritic plaques (arrows) with HD + low-dose AGO (H&E, 100x); (F) HD + high-dose AGO (H&E, 100x); (G) positive Congo Red staining showing astrocytic hyperplasia with reactive gliosis detected in all treated groups (Congo Red, 100x).

brain MT2 expression was also increased relative to controls by +62.5% and +137.5%, respectively [F (6, 49) = 284.188, $P < 0.0001$] (Fig. 12D).

In contrast, HD reduced brain MT2 by –57.5% [F (6, 49) = 284.188, $P < 0.0001$] (Fig. 12D), as was with ACh. While combined HD + low-dose AGO redeemed brain *MT2* to control

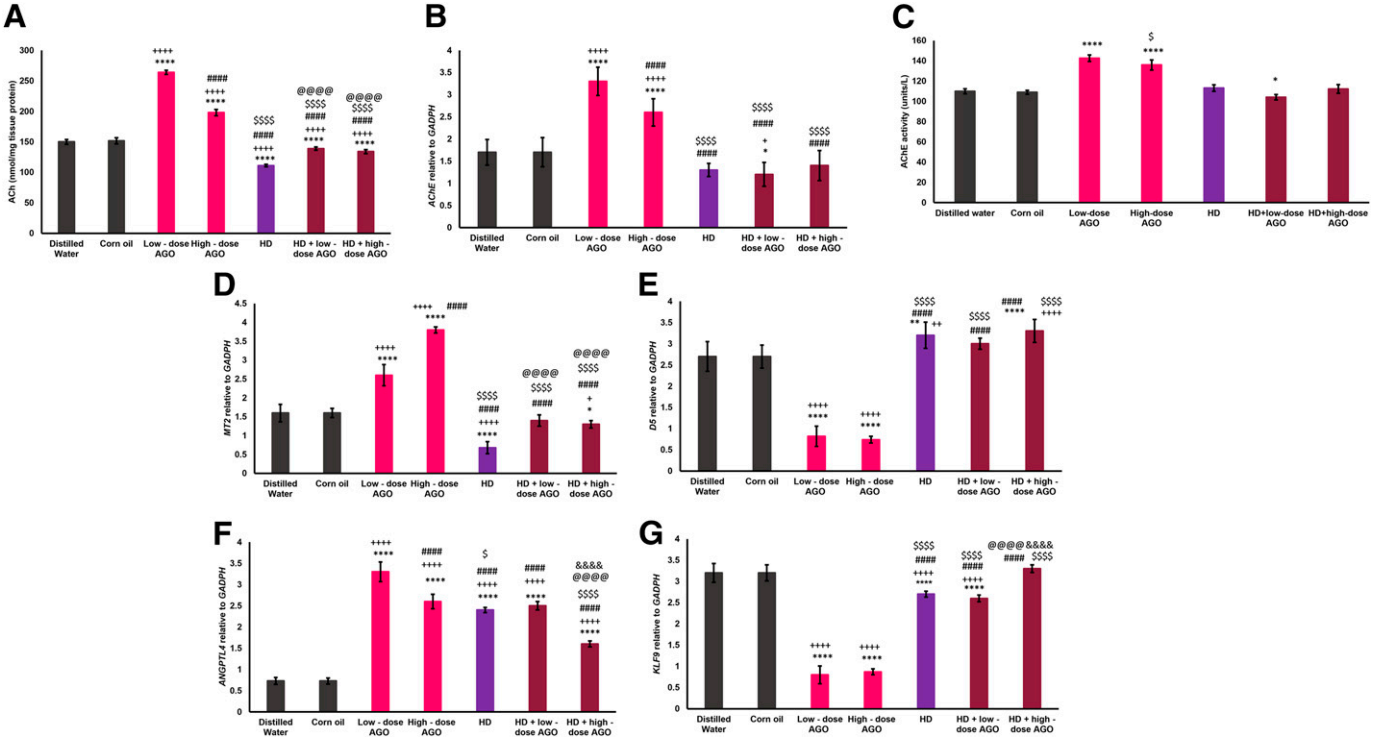

Fig. 12. Biochemical parameters in brain homogenate of adult male Wistar albino rats subdivided into control (oral DW or i.p. corn oil), low-dose AGO (oral 40 mg/kg), high-dose AGO (oral 80 mg/kg), HD (i.p. 4 mg/kg, once weekly), HD + low-dose AGO, and HD + high-dose AGO, showing (A) ACh level; (B) AChE; (C) AChE activity; (D) MT2; (E) D5; (F) ANGPTL4; (G) KLF9. Data are expressed as mean ± S.D. Significant when $P < 0.05$. $^{*}P < 0.05$, $^{**}P < 0.01$, $^{****}P < 0.0001$ compared with controls (DW). $^{+}P < 0.05$, $^{++}P < 0.01$, $^{++++}P < 0.0001$ compared with controls (corn oil). $^{\#\#\#\#}P < 0.0001$ compared with low-dose AGO. $^{\$}P < 0.05$, $^{\$\$\$\$}P < 0.0001$ compared with high-dose AGO. $^{@@@@}P < 0.0001$ compared with HD. $^{\&\&\&\&}P < 0.0001$ compared with HD + low-dose AGO.

level, HD + high-dose AGO displayed a persistently reduced brain *MT2* relative to controls by –18.75% [$F(6, 49) = 284.188$, $P = 0.018$] (Fig. 12D).

In contrast to brain acetylcholine, AChE, and MT2, brain D5 relative expression exhibited significant reductions with both AGO doses relative to controls by –69.63% and –72.59%, respectively [$F(6, 49) = 153.895$, $P < 0.0001$] (Fig. 12E).

Unlike AGO, HD increased brain D5 relative expression relative to controls by +18.52% [$F(6, 49) = 153.895$, $P = 0.004$] (Fig. 12E), in contrast to its effect on brain MT2. While HD + low-dose AGO redeemed brain *D5* expression to control levels, HD + high-dose AGO exhibited a persistently higher brain D5 compared with controls by +22.22% [$F(6, 49) = 153.895$, $P < 0.0001$] (Fig. 12E).

HD+ High-Dose AGO Was the Least to Increase Brain ANGPTL4 While Redeeming Brain KLF9 to Control Level. Compared with controls, the relative expression of brain ANGPTL4 was increased with both AGO doses by +352.06% and +256.16%, respectively [$F(6, 49) = 500.816$, $P < 0.0001$] as well as with HD by +228.77% [$F(6, 49) = 500.816$, $P < 0.0001$] (Fig. 12F).

Such brain ANGPTL4 increase was not redeemed with either HD +low-dose AGO or HD + high-dose AGO to exceed control levels by +242.47% and +119.18%, respectively [$F(6, 49) = 500.816$, $P < 0.0001$], more obvious when low-dose AGO was used in combination (Fig. 12F).

Unlike brain ANGPTL4, both AGO doses as well as HD reduced brain *KLF9* expression relative to controls by –75%, –72.81%, and –15.63%, respectively [$F(6, 49) = 437.511$, $P < 0.0001$] (Fig. 12G).

While HD + low-dose AGO displayed a persistently lower brain KLF9 relative to controls by –18.75% [$F(6, 49) = 437.511$, $P < 0.0001$], HD + high-dose AGO redeemed brain KLF9 to control levels (Fig. 12G). A descriptive summary of the study findings is provided in Table 2.

Total EEG Power Was Positively Correlated with Brain MT2 While TpTe Was Negatively Correlated to AChE Activity and Brain ANGPTL4 Was Negatively Correlated with KLF9

Total EEG power was positively correlated to brain MT2 receptors expression ($r = 0.83$, $P = 0.040$) (Fig. 13A). TpTe was negatively correlated to AChE activity ($r = –0.69$, $P < 0.0001$) (Fig. 13B). The weight of each of the right and left brain hemisphere was negatively correlated to AChE activity ($r = –0.56$, $r = –0.72$, respectively, $P < 0.0001$) (Fig. 13C).

AChE activity was positively correlated to ACh level ($r = 0.53$, $P < 0.0001$) and AChE expression ($r = 0.65$, $P < 0.0001$) (Fig. 13D). Conversely, AChE activity was negatively correlated to brain D5 ($r = –0.60$, $P < 0.0001$). (Fig. 13E). While AChE activity was positively correlated to ANGPTL4 ($r = 0.51$, $P < 0.0001$), it was negatively correlated to brain KLF9 ($r = –0.52$, $P < 0.0001$) (Fig. 13F).

The brain level of ACh was positively correlated to brain MT2 ($r = 0.94$, $P = 0.005$), while negatively correlated to brain D5 ($r = –0.93$, $P = 0.007$) (Fig. 13G). The brain MT2 was negatively correlated to brain *D5* ($r = –0.99$, $P < 0.0001$) (Fig. 13H). Brain ANGPTL4 was negatively correlated to brain KLF9 ($r = –0.94$, $P = 0.005$) (Fig. 13I).

Discussion

To our knowledge, this is the first study to address the cognitive impact of chronic HD combined with AGO, compared with either drug. Our work discriminated between two AGO doses (40 mg/kg and 80 mg/kg) commonly employed in previous research work. As HD releases active haloperidol, our discussion included the studies on both HD and haloperidol, the latter being the more extensively studied. The selection of male rats matched the reports highlighting a better performance of males when assessing visual-spatial tasks (McCarrey et al., 2016) employed herein. In clinical settings, one of the major indications for the use of HD is schizophrenia, which is more prevalent in males (X. Li et al., 2022). Avoiding the effects of fluctuating hormones during estrus cycles and potential effects on some of the assessed signaling mechanisms (Gunn et al., 2016; Spencer et al., 2008; Zachry et al., 2021), the male gender was chosen.

In agreement with the lack of cognitive alteration with prolonged corn oil intake in control rats, a randomized controlled trial reported a similar lack of additional benefit after 6-month corn oil intake in subjects with normal cognition (Maltais et al., 2022). However, other studies demonstrated improved cognition following alternate-day intraperitoneal injection of corn oil to a mouse model of Down syndrome after 30 days (Giacomini et al., 2018) or when corn oil, supplemented by other vitamins, was consumed by humans (Gutierrez et al., 2021).

In this study, the cognitive improvement observed with HD + high-dose AGO could be attributed to enhanced dopaminergic signaling (Speranza et al., 2021). The involvement of the MT2/D5 interplay is plausible, given the concomitant reduction in brain MT2 against D5 upregulation, further supported by the negative correlation between MT2 and D5, corroborating the inhibitory effect of melatonin over dopamine signaling through D1 and D2 receptors (Sweis, 2005). Furthermore, the positive correlation between brain ACh and MT2 versus the negative correlation linking ACh to D5 was in partial agreement with a reduced brain ACh, relieving the disinhibition of dopaminergic neurons and subsequently enhancing dopamine release (Exley & Cragg, 2008). Based on the assumption that a "cholinergic-melatonergic-dopaminergic trialogue" exists in the context of cognition, we hypothesized that the concomitantly reduced brain ACh and downregulated MT2, subsequently upregulating brain D5, might enhance some aspects of cognition, complementary to the cholinergic dysfunction hypothesis, which could involve other aspects of cognition, depending on the disordered function in context. The involvement of noncholinergic pathways was supported herein when opposite neurochemical changes observed with both AGO doses precipitated some cognitive impairment. In the presence of similar ACh, MT2, and D5 changes as HD + high-dose AGO, such cognitive impairment was not evident with HD, despite showing the most extensive neuropathologic affection. Thus, the cholinergic-melatonergic-dopaminergic trialogue we hypothesized could be the basis to explore novel pharmacologic targets, offering diverse therapeutic alternatives that might not only fill major cognitive gaps between normal individuals but also ameliorate resistant cases to the currently available cognitive enhancers.

TABLE 2
Descriptive summary of the main findings, studying adult male Wistar albino rats subdivided into control (oral DW or i.p. corn oil), low-dose AGO (oral 40 mg/kg), high-dose AGO (oral 80 mg/kg), HD (i.p. 4 mg/kg, once weekly), HD + low-dose AGO, and HD + high-dose AGO

Groups Assessments	Low-Dose AGO	High-Dose AGO	HD	HD + Low-Dose AGO	HD + High-Dose AGO
Dim to bright light preference					
Latency	↓	↑	Unaffected	Unaffected	↑
Percent time spent in bright light	↑	Unaffected	↑	↑	↑
Percent time spent in dim light	↓	Unaffected	Unaffected	↓	↓
Y-maze test					
Number of alternations	Unaffected	Unaffected	Unaffected	Unaffected	Unaffected
Percent of alternations	↓	↓	Unaffected	Unaffected	↑
EEG					
Total EEG power	Unaffected	Unaffected	Unaffected	Unaffected	Unaffected
Total beta power	Unaffected	↑	Unaffected	Unaffected	Redeemed
Total delta power	Unaffected	Unaffected	Unaffected	Unaffected	Unaffected
Mean power frequency source	Unaffected	Unaffected	↑	Redeemed	↓
Mean power frequency beta	Unaffected	Unaffected	Unaffected	Unaffected	Unaffected
Mean power frequency delta	↓	Unaffected	Unaffected	Redeemed	Unaffected
Mean amplitude	Unaffected	↑	↑	↑	Redeemed
Polarity of source wave	Unaffected	Inverted (Positive)	Inverted (Positive)	Redeemed	Redeemed
Mean amplitude beta	Unaffected	↑	Unaffected	Unaffected	Redeemed
Polarity of beta wave	Inverted (Negative)	Unaffected	Unaffected	Inverted (Negative)	Redeemed
Mean amplitude delta	Unaffected	↑	↑	↑	Redeemed
Polarity of delta wave	Unaffected	Inverted (Positive)	Inverted (Positive)	Inverted (Positive)	Redeemed
ECG					
Heart rate	Unaffected	↓	↓	Redeemed	Redeemed
P duration	↓	↓	↓	↓	↓
P amplitude	Unaffected	↓	↓	↓	Redeemed
Polarity of P wave	Unaffected	Unaffected	Inverted	Inverted	Inverted
PR interval	↓	↓	↓	Redeemed	↓
R amplitude	↑	↑	↑	↑	↑
S amplitude	↓	Unaffected	↓	↓	Redeemed
S wave direction	Unaffected	Unaffected	Unaffected	Inverted upwards	Unaffected
QRS interval	↓	Unaffected	Unaffected	Redeemed	Unaffected
QTc	↓	↓	↓	↓	Redeemed
ST amplitude	↑	Unaffected	Unaffected	Redeemed	↑
ST direction	Elevated	Depressed	Elevated	Elevated	Depressed
JT	↓	↓	↓	Redeemed	Redeemed
T wave amplitude	Unaffected	Unaffected	Unaffected	Unaffected	↑
T wave inversion	Unaffected	Unaffected	Unaffected	Unaffected	Inverted
TpTe	↓	↓	Unaffected	Redeemed	Redeemed
RR	Unaffected	↑	↑	Redeemed	↑
Body and brain weights					
Body weight	Unaffected	Unaffected	Unaffected	↑	Unaffected
Weight of the right brain-hemisphere	↓	↓	Unaffected	Redeemed	Redeemed
Weight of the left brain-hemisphere	↓	↓	Unaffected	Redeemed	Redeemed
Brain pathology					
Inflammatory cellular infiltrate		Mild to moderate			
Fascicular edema	Mild	Mild	Moderate	Mild	Mild
Astrocytic hyperplasia	Yes	Yes	Yes	Yes	Minimal
Reactive gliosis	Yes	Yes	Yes	Yes	Minimal
Neuritic plaques	Scarce	Scarce	Frequent	Few	
Neurofibrillary tangles	Scarce		Scattered	Scattered	
Beta-amyloid plaques					
ABC score	A0B1C1	A0B0C1	A0B1C2	A0B1C1	A0B0C0
Brain biochemical analysis					
ACh level	↑	↑	↓	↓	↓
AChE catalytic activity	↑	↑	Unaffected	↓	Redeemed
Gene expression relative to *GAPDH*					
AChE	↑	↑	Unaffected	↓	Redeemed
MT2	↑	↑	↓	Redeemed	↓
D5	↓	↓	↑	Redeemed	↑
ANGPTL4	↑	↑	↑	↑	↑
KLF9	↓	↓	↓	↓	Redeemed

Data provided involves comparison with control rats receiving DW.
↑ Increase; ↓ Decrease.

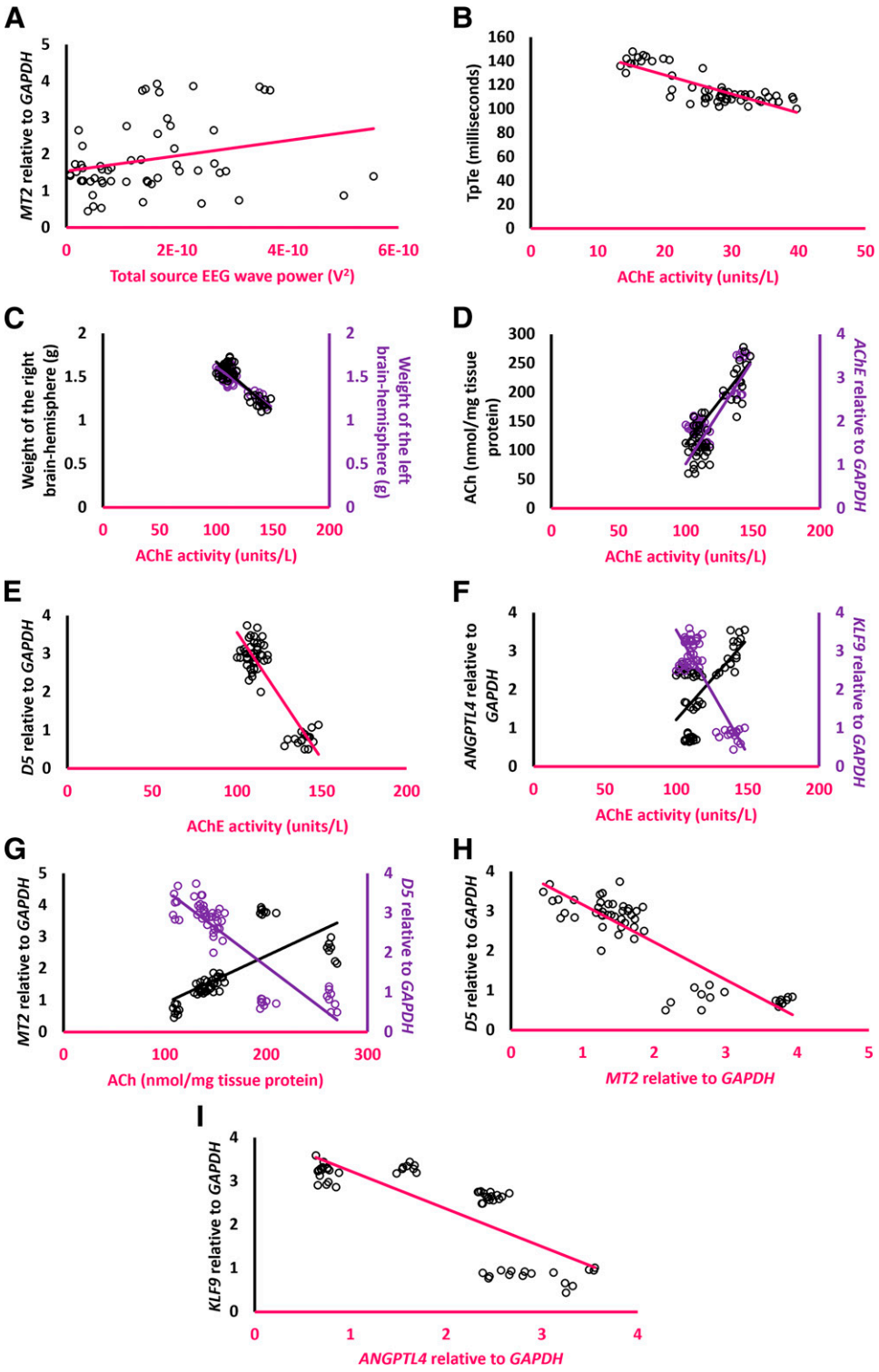

Fig. 13. Scatter plots showing correlations between (A) total EEG power and MT2 expression ($r = 0.83$, $P = 0.040$); (B) TpTe and AChE activity ($r = -0.69$, $P < 0.0001$); (C) the weight of each of the right and left brain hemisphere and AChE activity ($r = -0.56$, $r = -0.72$, respectively, $P < 0.0001$); (D) AChE activity and each of ACh level and *AChE* expression ($r = 0.53$, $r = 0.65$, respectively, $P < 0.0001$); (E) AChE activity and *D5* expression ($r = -0.60$, $P < 0.0001$); (F) AChE activity and each of *ANGPTL4* and *KLF9* expression ($r = 0.51$, $r = -0.52$, respectively, $P < 0.0001$); (G) ACh and each of *MT2* ($r = 0.94$, $P = 0.005$) and *D5* expression ($r = 0.93$, $P = 0.007$); (H) *D5* and *MT2* expressions ($r = -0.99$, $P < 0.0001$); (I) *ANGPTL4* and *KLF9* expressions ($r = -0.94$, $P = 0.005$). *Spearman rho*. Significant when $P < 0.05$.

We extended our cholinergic-melatonergic-dopaminergic trialogue to ANGPTL4 and KLF9, being essential targets in the issue of distorted brain microstructure (Zheng et al., 2021). To our knowledge, no previous studies have assessed the effects of prolonged treatment with HD, AGO, and their combination on brain ANGPTL4 and KLF9 in the context of cognition. We found that the HD + high-dose AGO was the least to induce ANGPTL4 expression but, more importantly, without altering

KLF9 expression, unlike the other treated groups, in which KLF9 was downregulated. Thus, our study proposed the implication of KLF9 deficiency in cognitive disorders, as was with KLF2 in the mouse model of AD and in humans (Fang et al., 2017; Wu et al., 2013). The negative correlation between ANGPTL4 and KLF9 highlighted their inverse relationship in the context of cognition (Shuff et al., 2021), after previous studies detected elevated ANGPTL4 in postmortem specimens of patients with AD (Yan et al., 2019) and its association with poor prognosis of ischemic stroke (Zheng et al., 2021).

The relatively less cognitive improvement observed with HD + low-dose AGO could be attributed to worse neuropathologic features and different neurochemical alterations, lacking similar MT2 and D5 changes as HD + high-dose AGO, added to a more extensive ANGPTL4 upregulation against a downregulated KLF9, reinforcing the cholinergic-melatonergic-dopaminergic trialogue and the feasibility to explore noncholinergic targets for cognitive dysfunction (Doraiswamy, 2002; Petrikis et al., 2004). The exclusive increase in body weight with HD + low-dose AGO might have also contributed, based on previous studies linking obesity to reduced cognition (Buie et al., 2019; T. Li et al., 2022). Though not the focus of this work, it is interesting to mention that HD + low-dose AGO was the only treatment regimen associated with a downregulated brain AChE expression and reduced catalytic activity, emphasizing the negative correlation between AChE and body mass index reported in a recent study involving female university students (Hamouda et al., 2019). It is noteworthy to highlight that reduced ACh occurred, despite a downregulated AChE. So whether this is some sort of protective compensatory mechanism to arrest the progression of cholinergic deficiency (Brown, 2019) requires further elaborative research work and, if proven, could rationalize the lack of efficacy of anticholinesterases in some cases of cognitive impairment. In our study, the positive correlation linking AChE activity and the brain ACh level could validate such a compensatory relationship.

In our model, the slight cognitive amelioration following prolonged HD administration was associated with increased mean power of source wave frequency, so that the power spectral density of the source wave was maximum at a frequency corresponding to the fast gamma range (60–100 Hz) (Colgin, 2016), linked to enhanced memory and learning in previous mice models (Sharpe et al., 2020; Zheng et al., 2016). Although HD induced almost similar neurochemical alteration as HD + high-dose AGO, one of the major differences was KLF9 downregulation; the other was the extensive AD-like features. In a previous rodent model, daily intramuscular injection of haloperidol (1.5 mg/kg) for 28 days induced neurodegenerative changes in the striatum and hippocampus (Polydoro et al., 2004), justifying the less cognitive impairment seen with HD, relative to acute intraperitoneal haloperidol injection (0.05 mg/kg) in rotenone-treated neonatal male Wistar rats (Varga et al., 2021). Nonetheless, the effect of HD on cognition seems controversial (Lalonde & Strazielle, 2017).

Both AGO doses improved some cognitive features and worsened others. The improvement of some cognitive indices using AGO agreed with previous studies Navarro-Francés and Arenas, 2014; Rao Barkur and Bairy, 2015; Meseguer Henarejos et al., 2020). The associated increased brain ACh, if supporting the cognitive improvement, could not justify the featured cognitive dysfunction, except after applying the hypothetical cholinergic-noncholinergic crosstalk, in which the concomitantly increased ACh and upregulated MT2, subsequently downregulating D5, added to the inclusion of ANGPTL4 upregulation, against KLF9 downregulation are introduced as novel co-players in the cognitive issue paradigm. Considering the inverse relationship between AChE activity on one side, enhanced herein, and brain D5 and KLF9 on the other side, as well as its positive link to ANGPTL4, AChE activity should be considered an independent factor in the cognitive dilemma. Elevated ACh activates presynaptic muscarinic receptors, thus suppressing the excitatory inputs needed for memory retrieval, leading to cognitive dysfunction (Hasselmo, 2006). Nonetheless, the concomitantly upregulated AChE expression along with enhanced catalytic activity highlighted its plausible protective role to maintain an optimum ACh level (Brown, 2019), thus justifying some concurrent cognitive improvement. The excess melatonergic precipitating cognitive dysfunction was previously supported by a phase IV clinical trial involving women above 60 years old who experienced memory impairment following 1 to 6 months of melatonin intake (Melatonin and Memory loss, a phase IV clinical study of FDA data - eHealthMe). In our experiment, such worsening did not occur with either HD, when MT2 was downregulated, or HD + low-dose AGO, when MT2 was redeemed to control levels. The associated reduced weight of the right and left brain hemispheres harmonized with the cognitive dysfunction and was in partial agreement to a previous correlation between brain size and both cognitive decline and dementia risk (Tan et al., 2017), possibly supporting the use of brain size as a surrogate marker to predict behavioral aspects of AD (Boublay et al., 2020). The inverse relationship linking the brain-hemispheric weights and AChE catalytic activity supports, in part, the therapeutic merit of anticholinesterases in neurodegenerative disorders, regardless of ACh level. It is worth mentioning that the brain weight might not be an accurate indicator though, based on the discrepancies between the changes of the weights of the brain hemispheres and the extent of neuropathology, as observed with HD. In contrast to our work, neither brain weights nor brain microstructure was changed when Yang et al. (2019) employed toxic AGO doses, but for a shorter duration of >28 days. The duration might be a crucial determinator, as in various disease models, short-term AGO did not provoke AD-like features (Yucel et al., 2016; Chanmanee et al., 2022).

The discrepancies between the treated groups could be also attributed to differences recovered on EEG recordings, impacting sleep (Zavecz et al., 2023), albeit this was not our focus. With low-dose AGO, a reduced mean power frequency delta wave was noticeable, seemingly reflecting an enhanced nonrapid eye movement previously detected in mice receiving the same AGO dose intraperitoneally for 21 days (Tchekalarova et al., 2020). The sleep-promoting ability of high-dose AGO was evident when total beta power was increased, being linked to a tranquilizing activity (Walker et al., 2001) and a sleep-like state (Fernandez-Mendoza et al., 2019), substantiated by concurrently increased delta amplitude (Kawai et al., 2016). With HD + low-dose AGO, the increased delta wave amplitude exceeded that observed with HD, indicating different sleep-promoting potentialities (Jones et al., 2014) and subsequent differential effects on cognition.

It is noteworthy to add some findings involving different epileptogenic activities that could not be overlooked, not only as part of the pharmacovigilance evaluation of HD-AGO combination but also due to their relevance, based on the link between epileptogenesis and both working memory impairment

(Arski et al., 2022) and the occurrence of dementia-like cognitive decline (Chin and Scharfman, 2013; Imfeld et al., 2013). In this context, the reduced mean power frequency of the source wave added to the undisturbed polarity of EEG waves detected with HD + high-dose AGO, exhibiting cognitive enhancement, highlighted a lower risk for epileptogenic activity (Kara et al., 2020), against the increased mean power frequency of source wave seen with HD, showing minimal cognitive improvement, reflected discrepant effects on cortical excitability (Barbiero et al., 2007; Ly et al., 2016) and varied potentialities for proconvulsant activity (Zhou and Li, 2020). Knowing that the EEG montage was uniform among all studied groups and that the source wave is likely to be negative as corresponding to superficial depolarizations using scalp electrodes, the inversion of negative to positive polarity observed in source and delta waves seen with HD, high-dose AGO and HD + low-dose AGO, might increase the likelihood of proconvulsive activity, with a possible link to reduced cognitive performance (Janati et al., 2013) or improvement, especially in the presence of AD-like neuropathologic features. Therefore, such epileptogenic activity contributed, in part, to the cognitive deterioration observed with high-dose AGO and the lack of substantial cognitive improvement with HD and HD + low-dose AGO. The implication of melatonin in provoking epileptogenesis was encountered previously in human cases (Sandyk et al., 1992; Sheldon, 1998) and was corroborated herein by detecting a positive correlation between brain MT2 and total EEG power, added to high-dose AGO displaying the highest source EEG wave amplitude in the presence of MT2 upregulation.

The brain-cardiac crosstalk was recently reported (Yamaguchi et al., 2020; Lin et al., 2022) and was demonstrated in patients who experienced myocardial injury following cerebral stroke (Krause et al., 2017). Similarly, manipulation of central neurotransmission can impact cardiorespiratory function (Díaz et al., 2021). In turn, cardiac ischemia might alter brain neurotransmission and trigger neuroinflammatory changes (Díaz et al., 2020), also impacting cognitive performance (Amorim et al., 2022; van Nieuwkerk et al., 2023). Therefore, ECG was recorded.

Our work is one of few studies investigating the impact of prolonged AGO administration on cardiac electrophysiology in a normal setting, while other studies and reviews evaluated the use of melatonin in managing cardiovascular diseases, employing animals and patients with disordered cardiac functions (Dominguez-Rodriguez, 2012; Sun et al., 2016; Nduhirabandi and Maarman, 2018).

In this study, while all treatments triggered changes indicative of cardiac ischemia and arrhythmia, it is worth mentioning that the most extensive ECG alterations were observed with both AGO doses, possibly rationalizing the concurrent cognitive dysfunction. Exclusively, reduced TpTe interval, indicating reduced time for transmural dispersion of ventricular repolarization (Opthof et al., 2009), was evident with both AGO doses. Interestingly, the catalytic activity of brain AChE, enhanced with both AGO doses, was negatively correlated to TpTe. When such AChE activity was reduced or unaltered, TpTe was unaffected. A thorough literature search did not reveal studies outlining the significance of short TpTe nor its correlation to central AChE activity. Most studies focused on TpTe prolongation as a risk of ventricular tachycardia and fibrillation (Zumhagen et al., 2016; Tse et al., 2017). As late sodium channels or sodium-calcium exchange are important determinants of TpTe interval (Antzelevitch, 2007), the occurrence of channelopathies or electrolyte imbalances could have provoked such an acceleration. Recently, a case report published in 2022 (Siao et al., 2022) suggested a causal relationship between AGO and cardiac arrhythmias, supporting the AGO-triggered cardiac electrical events found in our work. In male and female rats administered 28 days of oral daily AGO at doses of 200, 400, and 800 mg/kg, exceeding the doses used in clinical settings, there was no evidence for microstructural cardiac abnormalities (Yang et al., 2019). The ECG disturbances detected herein should be further weighed against some of the recently claimed vascular benefits of AGO when administered to female Wistar rat models of lipopolysaccharide-induced endothelial injury (Asci et al., 2022).

Contrasting low- to high-dose AGO, the former reduced QRS duration and was associated with elevated ST; the latter reduced P wave amplitude, prolonged RR interval, and slowed HR. The slowed HR associated with prolonged RR interval suggests a sinus node or autonomic dysfunction, triggering bradycardia and recurrence of atrial fibrillation (AF) (Amasyali et al., 2014). RR was adopted also as a prognostic marker in patients with AF (Zyśko et al., 2021); in turn, AF can provoke bradycardia (Barrett et al., 2012). The reduced P wave amplitude, denoting reduced atrial contractility, can also be associated with a higher risk for AF, added to heart failure (Park et al., 2016; Ostrowska et al., 2022; Zhang et al., 2023). ST elevation reflected the possibility of cardiac ischemia (Coppola et al., 2013). Reduced QRS interval, corresponding to accelerated inter- or intraventricular conduction, together with ST elevation, albeit denoting apparently favorable enhanced ventricular conduction and early repolarization, as previously published in case reports by (Wolpert et al., 2008), the clinicians were advised to be cautious as these EEG features might denote abnormal sodium channels disorders or increased Purkinjie fibers penetrating deep into the myocardium.

The ECG changes observed with HD were, seemingly, akin to those seen with high-dose AGO; however, inverted P wave, elevated ST, and prolonged QRS duration relative to high-dose AGO were superimposed. The inverted P wave could indicate a sinus node dysfunction or myocardial infarction (Khanna et al., 2022). The extensive ECG changes could have some clue to the worst neuropathology featured with HD (Shuff et al., 2021).

HD + AGO, regardless of AGO dose, triggered de novo ECG features, distinct from either HD or AGO monotherapy. HD + low-dose AGO caused a positive upstroke of S wave, while HD + high-dose AGO triggered a tall, inverted T wave, indicative of cardiac ischemia (Kashou et al., 2019).

Despite that combined HD + AGO redeemed many of the HD- and AGO-induced ECG changes, inverted P wave, observed with HD, and reduced P wave duration as well as tall R wave, seen with both HD and AGO, persisted. HD + low-but not high-dose AGO redeemed the reduced PR interval, as seen in the other treated groups. In turn, HD + high-but not low-dose AGO redeemed the reduced QTc seen in the other treated groups. The reduced P wave duration, denoting reduced atrial conductivity, can be also associated with a higher risk for AF and heart failure. The reduced PR interval, signifying an accelerated atrio-ventricular conduction, heightened AF risk, predisposing also to the potentially lethal ventricular fibrillation (Neshiewat et al., 2023). The increased R wave amplitude could highlight an increased blood mass inside the cardiac ventricles during early ventricular depolarization, predisposing to ventricular hypertrophy (Bonoris et al., 1978). A persistent tall R wave could denote myocardial

ischemia and/or bundle branch block (Sinno et al., 2008), both being previously documented as adverse events of haloperidol (Ter Bekke and Volders, 2020). Reduced QTc, reflecting accelerated cardiac repolarization, could occur secondary to channelopathies or electrolyte imbalances (https://www.acc.org/latest-in-cardiology/articles/2016/10/05/08/06/short-qt-syndrome), predisposing to arrhythmia (Anttonen et al., 2009).

Although no mortalities occurred, such adverse ECG changes should be weighed against the cognitive benefit when transitioning to clinical settings, given the higher risk of AF-related hospitalization in patients with heart failure and the substantial risk for morbidity and sudden cardiac death reported in patients with heart failure in case of arrhythmia (Masarone et al., 2017; Yuyun et al., 2023).

Limitations of the Study. Biochemical analysis did not include cardiac specimens. Liver function tests and electrolytes were not assessed.

Conclusion

HD + high-dose AGO displayed the best cognitive performance, matching the ameliorated neuropathology among treated groups, despite reduced brain ACh. HD + high-dose AGO was the least to alter the EEG recordings, scavenging the epileptogenic-like activity noticed with AGO and HD. HD + high-dose AGO was the least to increase brain ANGPTL4, redeeming brain AChE expression and activity to control levels, and exclusively resolving KLF9 downregulation. The arrhythmogenic and ischemic ECG abnormalities did not match such cognitive improvement.

Either low- or high-dose AGO exhibited a perplexed cognitive amelioration and worsening, against trivial cognitive improvement with HD. High-dose AGO exhibited epileptogenic activity on EEG more than low-dose AGO. Both AGO and HD provoked profound derangements of brain ACH, AChE, MT2, D5, ANGPTL4, and KLF9, along with AD-like neuropathologic features, extensive with HD. The disturbed brain microstructure as well as *MT2* and *D5* alterations were redeemed with HD + low-dose AGO, featuring some cognitive improvement but less than HD + high-dose AGO.

Based on our preclinical experiment, HD + high-dose AGO could offer a potential cognitive enhancer. Periodic ECG monitoring is recommended. Applying to female animals warrants further investigations. Exploring HD and other antipsychotics, combined to AGO, in models of dementia-triggered psychotic features and schizophrenia should be addressed. Further research work is required to elucidate the neurologic benefit versus cardiac risk of this combination in preclinical and clinical settings.

Acknowledgments

The authors thank Walaa M. Sayed, professor of anatomy and embryology, Faculty of Medicine, Kasr Al-Ainy, Cairo University, Cairo, Egypt, for editing the pathology images to comply with journal formatting and guidelines. They thank Editage (www.editage.com) for English-language editing.

Data Availability

The authors declare that all the data supporting the findings of this study are contained within the paper.

Authorship Contributions

Participated in research design: Abdelmissih.
Conducted experiments: Abdelmissih, Youssef.
Contributed new reagents or analytic tools: Abdelgwad, Ali, Negm.
Performed data analysis: Abdelgwad, Eshra.
Wrote or contributed to the writing of the manuscript: Abdelmissih, Abdelgwad, Ali, Negm, Eshra, Youssef.

References

Amasyali B, Kilic A, and Kilit C (2014) Sinus node dysfunction and atrial fibrillation: which one dominates? *Int J Cardiol* **175:**379–380.
Amorim S, Felício AC, Aagaard P, Suetta C, Blauenfeldt RA, and Andersen G (2022) Effects of remote ischemic conditioning on cognitive performance: A systematic review. *Physiol Behav* **254:**113893.
Anttonen O, Junttila J, Giustetto C, Gaita F, Linna E, Karsikas M, Seppänen T, Perkiömäki JS, Mäkikallio TH, Brugada R, et al. (2009) T-Wave morphology in short QT syndrome. *Ann Noninvasive Electrocardiol* **14:**262–267.
Antzelevitch C (2007) Role of spatial dispersion of repolarization in inherited and acquired sudden cardiac death syndromes. *Am J Physiol Heart Circ Physiol* **293:** H2024–H2038.
Arski ON, Wong SM, Warsi NM, Pang E, Kerr E, Smith ML, Taylor MJ, Dunkley BT, Ochi A, Otsubo H, et al. (2022) Epilepsy disrupts hippocampal phase precision and impairs working memory. *Epilepsia* **63:**2583–2596.
Asci H, Ozmen O, Erzurumlu Y, Sofu A, Icten P, and Kaynak M (2022) Agomelatine protects heart and aorta against lipopolysaccharide-induced cardiovascular toxicity via inhibition of NF-kβ phosphorylation. *Drug Chem Toxicol* **45:**133–142.
Barak S and Weiner I (2009) Towards an animal model of an antipsychotic drug-resistant cognitive impairment in schizophrenia: scopolamine induces abnormally persistent latent inhibition, which can be reversed by cognitive enhancers but not by antipsychotic drugs. *Int J Neuropsychopharmacol* **12:**227–241.
Barbiero VS, Giambelli R, Musazzi L, Tiraboschi E, Tardito D, Perez J, Drago F, Racagni G, and Popoli M (2007) Chronic antidepressants induce redistribution and differential activation of alphaCaM kinase II between presynaptic compartments. *Neuropsychopharmacology* **32:**2511–2519.
Barrett TW, Abraham RL, Jenkins CA, Russ S, Storrow AB, and Darbar D (2012) Risk factors for bradycardia requiring pacemaker implantation in patients with atrial fibrillation. *Am J Cardiol* **110:**1315–1321.
Baxter MG and Crimins JL (2018) Acetylcholine receptor stimulation for cognitive enhancement: better the devil you know? *Neuron* **98:**1064–1066.
Besnard A, Langberg T, Levinson S, Chu D, Vicidomini C, Scobie KN, Dwork AJ, Arango V, Rosoklija GB, Mann JJ, et al. (2018) Targeting Kruppel-like factor 9 in excitatory neurons protects against chronic stress-induced impairments in dendritic spines and fear responses. *Cell Rep* **23:**3183–3196.
Bonoris PE, Greenberg PS, Christison GW, Castellanet MJ, and Ellestad MH (1978) Evaluation of R wave amplitude changes versus ST-segment depression in stress testing. *Circulation* **57:**904–910.
Boublay N, Bouet R, Dorey J-M, Padovan C, Makaroff Z, Fédérico D, Gallice I, Barrellon M-O, Robert P, Moreaud O, et al.; Alzheimer's Disease Neuroimaging Initiative (2020) Brain volume predicts behavioral and psychological symptoms in Alzheimer's disease. *J Alzheimers Dis* **73:**1343–1353.
Brown DA (2019) Acetylcholine and cholinergic receptors. *Brain Neurosci Adv* **3:**2398212818820506.
Buie JJ, Watson LS, Smith CJ, and Sims-Robinson C (2019) Obesity-related cognitive impairment: the role of endothelial dysfunction. *Neurobiol Dis* **132:**104580.
Can ÖD, Üçel UI, Demir Özkay Ü, and Ulupõnar E (2018) The effect of agomelatine treatment on diabetes-induced cognitive impairments in rats: concomitant alterations in the hippocampal neuron numbers. *Int J Mol Sci* **19:**2461.
Chakraborty A, Kamermans A, van Het Hof B, Castricum K, Aanhane E, van Horssen J, Thijssen VL, Scheltens P, Teunissen CE, Fontijn RD, et al. (2018) Angiopoietin like-4 as a novel vascular mediator in capillary cerebral amyloid angiopathy. *Brain* **141:**3377–3388.
Chanmanee T, Wongpun J, Tocharus C, Govitrapong P, and Tocharus J (2022) The effects of agomelatine on endoplasmic reticulum stress related to mitochondrial dysfunction in hippocampus of aging rat model. *Chem Biol Interact* **351:**109703.
Chin J and Scharfman HE (2013) Shared cognitive and behavioral impairments in epilepsy and Alzheimer's disease and potential underlying mechanisms. *Epilepsy Behav* **26:**343–351.
Colgin LL (2016) Rhythms of the hippocampal network. *Nat Rev Neurosci* **17:** 239–249.
Coppola G, Carità P, Corrado E, Borrelli A, Rotolo A, Guglielmo M, Nugara C, Ajello L, Santomauro M, and Novo S; Italian Study Group of Cardiovascular Emergencies of the Italian Society of Cardiology (2013) ST segment elevations: always a marker of acute myocardial infarction? *Indian Heart J* **65:**412–423.
Debonnel G, Gaudreau P, Quirion R, and de Montigny C (1990) Effects of long-term haloperidol treatment on the responsiveness of accumbens neurons to cholecystokinin and dopamine: electrophysiological and radioligand binding studies in the rat. *J Neurosci* **10:**469–478.
Díaz HS, Andrade DC, Toledo C, Schwarz KG, Pereyra KV, Díaz-Jara E, Marcus NJ, and Del Rio R (2021) Inhibition of brainstem endoplasmic reticulum stress rescues cardiorespiratory dysfunction in high output heart failure. *Hypertension* **77:** 718–728.
Díaz HS, Toledo C, Andrade DC, Marcus NJ, and Del Rio R (2020) Neuroinflammation in heart failure: new insights for an old disease. *J Physiol* **598:**33–59.
Dominguez-Rodriguez A (2012) Melatonin in cardiovascular disease. *Expert Opin Investig Drugs* **21:**1593–1596.
Doraiswamy PM (2002) Non-cholinergic strategies for treating and preventing Alzheimer's disease. *CNS Drugs* **16:**811–824.
Durand-de Cuttoli R, Mondoloni S, Marti F, Lemoine D, Nguyen C, Naudé J, d'Izarny-Gargas T, Pons S, Maskos U, Trauner D, et al. (2018) Manipulating midbrain dopamine neurons and reward-related behaviors with light-controllable nicotinic acetylcholine receptors. *eLife* **7:**e37487.

Exley R and Cragg SJ (2008) Presynaptic nicotinic receptors: a dynamic and diverse cholinergic filter of striatal dopamine neurotransmission. *Br J Pharmacol* **153**(Suppl 1):S283–S297.
Fang X, Zhong X, Yu G, Shao S, and Yang Q (2017) Vascular protective effects of KLF2 on Aβ-induced toxicity: Implications for Alzheimer's disease. *Brain Res* **1663:**174–183.
Giacomini A, Stagni F, Emili M, Guidi S, Salvalai ME, Grilli M, Vidal-Sanchez V, Martinez-Cué C, and Bartesaghi R (2018) Treatment with corn oil improves neurogenesis and cognitive performance in the Ts65Dn mouse model of Down syndrome. *Brain Res Bull* **140:**378–391.
Gobbi G and Comai S (2019) Differential function of melatonin MT1 and MT2 receptors in REM and NREM sleep. *Front Endocrinol (Lausanne)* **10:**87.
Guermonprez L, Ducrocq C, and Gaudry-Talarmain YM (2001) Inhibition of acetylcholine synthesis and tyrosine nitration induced by peroxynitrite are differentially prevented by antioxidants. *Mol Pharmacol* **60:**838–846.
Gunn PJ, Middleton B, Davies SK, Revell VL, and Skene DJ (2016) Sex differences in the circadian profiles of melatonin and cortisol in plasma and urine matrices under constant routine conditions. *Chronobiol Int* **33:**39–50.
Gupta S, Singh P, Sharma BM, and Sharma B (2015) Neuroprotective effects of agomelatine and vinpocetine against chronic cerebral hypoperfusion induced vascular dementia. *Curr Neurovasc Res* **12:**240–252.
Gutierrez L, Folch A, Rojas M, Cantero JL, Atienza M, Folch J, Camins A, Ruiz A, Papandreou C, and Bulló M (2021) Effects of nutrition on cognitive function in adults with or without cognitive impairment: a systematic review of randomized controlled clinical trials. *Nutrients* **13:**3728.
Hamouda F, Ibrahim Abdu K, and Ibraheem M (2019) Study the relation between acetylcholinesterase and obesity in university students. *Int J Food Sci Nutr* **8:** 46–51.
Harmony T (2013) The functional significance of delta oscillations in cognitive processing. *Front Integr Nuerosci* **7:**83.
Hasselmo ME (2006) The role of acetylcholine in learning and memory. *Curr Opin Neurobiol* **16:**710–715.
He S, Jia H, Wu S, and Zhang X. (2017) Ameliorative effects of ginkgo biloba on haloperidol-induced vacuous chewing movement and BDNF plasm levels in rats: a dose-dependent effect. *Psychol Behav Sci* **3:**555643.
Hedges D, Farrer TJ, Bigler ED, Hopkins RO, Hedges D, Farrer TJ, Bigler ED, and Hopkins RO (2019). Cerebrovascular disease and cognition, in *The brain at risk,* Springer, Cham.
Hyman BT, Phelps CH, Beach TG, Bigio EH, Cairns NJ, Carrillo MC, Dickson DW, Duyckaerts C, Frosch MP, Masliah E, et al. (2012) National Institute on Aging-Alzheimer's Association guidelines for the neuropathologic assessment of Alzheimer's disease. *Alzheimers Dement* **8:**1–13.
Imfeld P, Bodmer M, Schuerch M, Jick SS, and Meier CR (2013) Seizures in patients with Alzheimer's disease or vascular dementia: a population-based nested case-control analysis. *Epilepsia* **54:**700–707.
Janati A, Talbi R, Klosen P, Mikkelsen JD, Magoul R, Simonneaux V, and El Ouezzani S (2013) Distribution and seasonal variation in hypothalamic RF-amide peptides in a semi-desert rodent, the jerboa. *J Neuroendocrinol* **25:**402–411.
Jang J-H, Kim J, Park G, Kim H, Jung E-S, Cha JY, Kim CY, Kim S, Lee J-H, and Yoo H (2019) Beta wave enhancement neurofeedback improves cognitive functions in patients with mild cognitive impairment: a preliminary pilot study. *Medicine (Baltimore)* **98:**e18357.
Jones SG, Riedner BA, Smith RF, Ferrarelli F, Tononi G, Davidson RJ, and Benca RM (2014) Regional reductions in sleep electroencephalography power in obstructive sleep apnea: a high-density EEG study. *Sleep (Basel)* **37:**399–407.
Kara SD, Amin U, and Benbadis SR (2020) Reversing the myth of phase reversals. *Expert Rev Neurother* **20:**3–5.
Kashou AH, May AM, DeSimone CV, Deshmukh AJ, Asirvatham SJ, Noseworthy PA (2019) Diffuse ST-segment depression despite prior coronary bypass grafting: An electrocardiographic-angiographic correlation. *J Electrocardiol* **55:**28–31.
Kawai M, Beaudreau SA, Gould CE, Hantke NC, Jordan JT, and O'Hara R (2016) Delta activity at sleep onset and cognitive performance in community-dwelling older adults. *Sleep (Basel)* **39:**907–914.
Khanna S, Sreedharan R, Trombetta C, and Bustamante S (2022) Inverted P waves: harmless or harbinger of doom? *Colombian J Anestesiol* **50**.
Krause T, Werner K, Fiebach JB, Villringer K, Piper SK, Haeusler KG, Endres M, Scheitz JF, and Nolte CH (2017) Stroke in right dorsal anterior insular cortex is related to myocardial injury. *Ann Neurol* **81:**502–511.
Lalonde R and Strazielle C (2017) Divergent effects of haloperidol on motor versus spatial functions. *Open J Parkinsons Dis Treat* **1:**032–038.
Li T, Qu J, Xu C, Fang T, Sun B, and Chen L (2022) Exploring the common gene signatures and pathogeneses of obesity with Alzheimer's disease via transcriptome data. *Front Endocrinol (Lausanne)* **13:**1072955.
Li X, Zhou W, and Yi Z (2022) A glimpse of gender differences in schizophrenia. *Gen Psychiatr* **35:**e100823.
Liang X, Huang Y, and Han X (2021) Associations between coronary heart disease and risk of cognitive impairment: a meta-analysis. *Brain Behav* **11:**e02108.
Lin CY, Lee CY, Lee HF, Wu MY, Tseng CN, Tsai FC, and Lin YH (2022) Postoperative stroke after type A aortic dissection repair: hemorrhage versus ischemia. *World J Surg* **46:**690–700
Doraiswamy PM (2002) Non-cholinergic strategies for treating and preventing Alzheimer's disease. *CNS Drugs* **16:**811–824.
Ly JQM, Gaggioni G, Chellappa SL, Papachilleos S, Brzozowski A, Borsu C, Rosanova M, Sarasso S, Middleton B, Luxen A, et al. (2016) Circadian regulation of human cortical excitability. *Nat Commun* **7:**11828.
Maltais M, de Souto Barreto P, Bowman GL, Smith AD, Cantet C, Andrieu S, Rolland Y, and Group MDS (2022) Omega-3 supplementation for the prevention of cognitive decline in older adults: does it depend on homocysteine levels? *J Nutr Health Aging* **26:**615–620.
Masarone D, Limongelli G, Rubino M, Valente F, Vastarella R, Ammendola E, Gravino R, Verrengia M, Salerno G, and Pacileo G (2017) Management of arrhythmias in heart failure. *J Cardiovasc Dev Dis* **4:**3.
McCarrey AC, An Y, Kitner-Triolo MH, Ferrucci L, and Resnick SM (2016) Sex differences in cognitive trajectories in clinically normal older adults. *Psychol Aging* **31:**166–175.
Meseguer Henarejos AB, Popović N, Bokonjić D, Morales-Delgado N, Alonso A, Caballero Bleda M, and Popović M (2020) Sex and time-of-day impact on anxiety and passive avoidance memory strategies in mice. *Front Behav Neurosci* **14:**68.
Miedel CJ, Patton JM, Miedel AN, Miedel ES, and Levenson JM (2017) Assessment of spontaneous alternation, novel object recognition and limb clasping in transgenic mouse models of amyloid-β and tau neuropathology. *J Vis Exp* **123:**e55523.
Mühlbauer V, Möhler R, Dichter MN, Zuidema SU, Köpke S, and Luijendijk HJ (2021) Antipsychotics for agitation and psychosis in people with Alzheimer's disease and vascular dementia. *Cochrane Database Syst Rev* **12:**CD013304.
Navarro-Francés CI and Arenas MC (2014) Influence of trait anxiety on the effects of acute stress on learning and retention of the passive avoidance task in male and female mice. *Behav Processes* **105:**6–14.
Nduhirabandi F and Maarman GJ (2018) Melatonin in heart failure: a promising therapeutic strategy? *Molecules* **23:**1819.
Nesheiwat Z, Goyal A, Jagtap M, Shammas A (2023) Atrial fibrillation (nursing), in *StatPearls [Internet]*, StatPearls Publishing, Treasure Island, FL.
Onaolapo OJ, Onaolapo AY, Mosaku TJ, Akanji OO, and Abiodun OR (2012) Elevated plus maze and Y-maze behavioral effects of subchronic, oral low dose monosodium glutamate in Swiss albino mice. *J Pharm Biol Sci* **3:**21–27.
Opthof T, Coronel R, and Janse MJ (2009) Is there a significant transmural gradient in repolarization time in the intact heart? Repolarization gradients in the intact heart. *Circ Arrhythm Electrophysiol* **2:**89–96.
Ostrowska B, Lind L, Sciaraffia E, and Blomström-Lundqvist C (2022) A short P-wave duration is associated with incident heart failure in the elderly: a 15 years follow-up cohort study. *J Geriatr Cardiol* **19:**643–650.
Park J-K, Park J, Uhm J-S, Joung B, Lee M-H, and Pak H-N (2016) Low P-wave amplitude (<0.1 mV) in lead I is associated with displaced inter-atrial conduction and clinical recurrence of paroxysmal atrial fibrillation after radiofrequency catheter ablation. *Europace* **18:**384–391.
Perini G, Della-Bianca V, Politi V, Della Valle G, Dal-Pra I, Rossi F, and Armato U (2002) Role of p75 neurotrophin receptor in the neurotoxicity by β-amyloid peptides and synergistic effect of inflammatory cytokines. *J Exp Med* **195:**907–918.
Petrikis P, Andreou C, Piachas A, Bozikas VP, and Karavatos A (2004) Treatment of Huntington's disease with galantamine. *Int Clin Psychopharmacol* **19:**49–50.
Pillai JA and Leverenz JB (2017) Sleep and neurodegeneration: a critical appraisal. *Chest* **151:**1375–1386.
Pollak NM, Hoffman M, Goldberg IJ, and Drosatos K (2018) Krüppel-like factors: crippling and un-crippling metabolic pathways. *JACC Basic Transl Sci* **3:**132–156.
Polydoro M, Schröder N, Lima MNM, Caldana F, Laranja DC, Bromberg E, Roesler R, Quevedo J, Moreira JCF, and Dal-Pizzol F (2004) Haloperidol- and clozapine-induced oxidative stress in the rat brain. *Pharmacol Biochem Behav* **78:**751–756.
Rao Barkur R and Bairy LK (2015) Evaluation of passive avoidance learning and spatial memory in rats exposed to low levels of lead during specific periods of early brain development. *Int J Occup Med Environ Health* **28:**533–544.
Rizzi G and Tan KR (2017) Dopamine and acetylcholine, a circuit point of view in Parkinson's disease. *Front Neural Circuits* **11:**110.
Roghani M, Joghataie MT, Jalali MR, and Baluchnejadmojarad T (2006) Time course of changes in passive avoidance and Y-maze performance in male diabetic rats. *Iran Biomed J* **10:**99–104.
Sandyk R, Tsagas N, and Anninos PA (1992) Melatonin as a proconvulsive hormone in humans. *Int J Neurosci* **63:**125–135.
Sharpe RLS, Mahmud M, Kaiser MS, and Chen J (2020) Gamma entrainment frequency affects mood, memory and cognition: an exploratory pilot study. *Brain Inform* **7:**17.
Sheldon SH (1998) Pro-convulsant effects of oral melatonin in neurologically disabled children. *Lancet* **351:**1254.
Shuff S, Oyama Y, Walker L, and Eckle T (2021) Circadian angiopoietin-like-4 as a novel therapy in cardiovascular disease. *Trends Mol Med* **27:**627–629.
Siao W-H, Cheng S, and Huang C-C (2022) Agomelatine potentially triggers cardiac arrhythmia: a case report. *J Clin Psychopharmacol* **42:**99–101.
Sinno MC, Kowalski M, Kenigsberg DN, Krishnan SC, and Khanal S (2008) R-wave amplitude changes measured by electrocardiography during early transmural ischemia. *J Electrocardiol* **41:**425–430.
Spencer JL, Waters EM, Romeo RD, Wood GE, Milner TA, and McEwen BS (2008) Uncovering the mechanisms of estrogen effects on hippocampal function. *Front Neuroendocrinol* **29:**219–237.
Speranza L, di Porzio U, Viggiano D, de Donato A, and Volpicelli F (2021) Dopamine: the neuromodulator of long-term synaptic plasticity, reward and movement control. *Cells* **10:**735.
Sun H, Gusdon AM, and Qu S (2016) Effects of melatonin on cardiovascular diseases: progress in the past year. *Curr Opin Lipidol* **27:**408–413.
Sweis D (2005) The uses of melatonin. *Arch Dis Child Educ Pract Ed* **90:**ep74–ep77.
Tan ZS, Spartano NL, Beiser AS, DeCarli C, Auerbach SH, Vasan RS, and Seshadri S (2017) Physical activity, brain volume, and dementia risk: the Framingham study. *J Gerontol A Biol Sci Med Sci* **72:**789–795.
Tchekalarova J, Kortenska L, Ivanova N, Atanasova M, and Marinov P (2020) Agomelatine treatment corrects impaired sleep-wake cycle and sleep architecture and increases MT_1 receptor as well as BDNF expression in the hippocampus during the subjective light phase of rats exposed to chronic constant light. *Psychopharmacology (Berl)* **237:**503–518.
Ter Bekke RMA and Volders PGA (2020) Haloperidol and sudden death in first acute myocardial infarction. *Int J Cardiol Heart Vasc* **26:**100482.
Tse G, Gong M, Wong WT, Georgopoulos S, Letsas KP, Vassiliou VS, Chan YS, Yan BP, Wong SH, Wu WKK, et al. (2017) The T_{peak}-T_{end} interval as an

electrocardiographic risk marker of arrhythmic and mortality outcomes: a systematic review and meta-analysis. *Heart Rhythm* **14:**1131–1137.
van Nieuwkerk AC, Delewi R, Wolters FJ, Muller M, Daemen M, and Biessels GJ; Heart-Brain Connection Consortium (2023) Cognitive impairment in patients with cardiac disease: implications for clinical practice. *Stroke* **54:**2181–2191.
Varga TG, de Toledo Simões JG, Siena A, Henrique E, da Silva RCB, Dos Santos Bioni V, Ramos AC, and Rosenstock TR (2021) Haloperidol rescues the schizophrenia-like phenotype in adulthood after rotenone administration in neonatal rats. *Psychopharmacology (Berl)* **238:**2569–2585.
Veronesi VB, Pioli MR, de Souza DN, Teixeira CJ, Murata GM, Santos-Silva JC, Hecht FB, Vicente JM, Bordin S, and Anhê GF (2021) Agomelatine reduces circulating triacylglycerides and hepatic steatosis in fructose-treated rats. *Biomed Pharmacother* **141:**111807.
Walker D, Mahoney C, Ilivitsky V, and Knott VJ (2001) Effects of haloperidol pretreatment on the smoking-induced EEG/mood activation response profile. *Neuropsychobiology* **43:**102–112.
Wang J-W, David DJ, Monckton JE, Battaglia F, and Hen R (2008) Chronic fluoxetine stimulates maturation and synaptic plasticity of adult-born hippocampal granule cells. *J Neurosci* **28:**1374–1384.
Wolpert C, Veltmann C, Schimpf R, Antzelevitch C, Gussak I, and Borggrefe M (2008) Is a narrow and tall QRS complex an ECG marker for sudden death? *Heart Rhythm* **5:**1339–1345.
Wu C, Li F, Han G, and Liu Z (2013) Aβ(1-42) disrupts the expression and function of KLF2 in Alzheimer's disease mediated by p53. *Biochem Biophys Res Commun* **431:**141–145.
Xu W, Tan C-C, Zou J-J, Cao X-P, and Tan L (2020) Sleep problems and risk of all-cause cognitive decline or dementia: an updated systematic review and meta-analysis. *J Neurol Neurosurg Psychiatry* **91:**236–244.
Yamaguchi T, Sumida TS, Nomura S, Satoh M, Higo T, Ito M, Ko T, Fujita K, Sweet ME, Sanbe A, et al. (2020) Cardiac dopamine D1 receptor triggers ventricular arrhythmia in chronic heart failure. *Nat Commun* **11:**4364.
Yan Q, He B, Hao G, Liu Z, Tang J, Fu Q, and Jiang CX (2019) KLF9 aggravates ischemic injury in cardiomyocytes through augmenting oxidative stress. *Life Sci* **233:**116641.
Yang Q, Zhou X, Li J, Ma Y, Lu L, Xiong J, Xu P, Li Y, Chen Y, Gu W, et al. (2019) Sub-acute oral toxicity of a novel derivative of agomelatine in rats in a sex-dependent manner. *Front Pharmacol* **10:**242.
Yohn CN, Gergues MM, and Samuels BA (2017) The role of 5-HT receptors in depression. *Mol Brain* **10:**28.
Yucel A, Yucel N, Ozkanlar S, Polat E, Kara A, Ozcan H, and Gulec M (2016) Effect of agomelatine on adult hippocampus apoptosis and neurogenesis using the stress model of rats. *Acta Histochem* **118:**299–304.
Yuyun MF, Kinlay S, Singh JP, and Joseph J (2023) Are arrhythmias the drivers of sudden cardiac death in heart failure with preserved ejection fraction? A review. *ESC Heart Fail* **10:**1555–1569.
Zachry JE, Nolan SO, Brady LJ, Kelly SJ, Siciliano CA, and Calipari ES (2021) Sex differences in dopamine release regulation in the striatum. *Neuropsychopharmacology* **46:**491–499.
Zavecz Z, Shah VD, Murillo OG, Vallat R, Mander BA, Winer JR, Jagust WJ, and Walker MP (2023) NREM sleep as a novel protective cognitive reserve factor in the face of Alzheimer's disease pathology. *BMC Med* **21:**156.
Zhang ZR, Ragot D, Massin SZ, Suszko A, Ha AC, Singh SM, and Chauhan VS (2023) P-wave duration-amplitude ratio quantifies atrial low-voltage area and predicts atrial arrhythmia recurrence following pulmonary vein isolation. *Can J Cardiol* **39:**1421–1431.
Zheng C, Bieri KW, Hwaun E, and Colgin LL (2016) Fast gamma rhythms in the hippocampus promote encoding of novel object–place pairings. *eNeuro* **3:**ENEURO.0001-16.2016.
Zheng X, Shen S, Wang A, Zhu Z, Peng Y, Peng H, Zhong C, Guo D, Xu T, Chen J, et al. (2021) Angiopoietin-like protein 4 and clinical outcomes in ischemic stroke patients. *Ann Clin Transl Neurol* **8:**687–695.
Zhou D and Li X (2020) Epilepsy EEG signal classification algorithm based on improved RBF. *Front Neurosci* **14:**606.
Zhu P, Goh YY, Chin HFA, Kersten S, and Tan NS (2012) Angiopoietin-like 4: a decade of research. *Biosci Rep* **32:**211–219.
Zumhagen S, Zeidler EM, Stallmeyer B, Ernsting M, Eckardt L, and Schulze-Bahr E (2016) Tpeak-Tend interval and Tpeak-Tend/QT ratio in patients with Brugada syndrome. *Europace* **18:**1866–1872.
Zyśko D, Persson A, Obremska M, Leśkiewicz M, Fedorowski A, Sutton R, and Johnson LS (2021) The importance of the longest R-R interval on 24-hour electrocardiography for mortality prediction in patients with atrial fibrillation. *Kardiol Pol* **79:**311–318.

Address correspondence to: Sherine Abdelmissih, Department of Medical Pharmacology, Faculty of Medicine, Kasr Al-Ainy, Cairo University, 182 Shobra Street, Shobra Misr, Cairo, Egypt. E-mail: Drshery_wa@yahoo.com, drshery_wa@kasralainy.edu.eg